# SANDIA REPORT

SAND2018-1900
Unlimited Release
Printed February 2018

# Removal of Stationary Sinusoidal Noise from Random Vibration Signals

Brian K. Johnson, Jerome S. Cap

Prepared by
Sandia National Laboratories
Albuquerque, New Mexico 87185 and Livermore, California 94550

Sandia National Laboratories is a multimission laboratory managed and operated by National Technology and Engineering Solutions of Sandia, LLC, a wholly owned subsidiary of Honeywell International, Inc., for the U.S. Department of Energy's National Nuclear Security Administration under contract DE-NA0003525.

Issued by Sandia National Laboratories, operated for the United States Department of Energy by National Technology and Engineering Solutions of Sandia, LLC.

**NOTICE:** This report was prepared as an account of work sponsored by an agency of the United States Government. Neither the United States Government, nor any agency thereof, nor any of their employees, nor any of their contractors, subcontractors, or their employees, make any warranty, express or implied, or assume any legal liability or responsibility for the accuracy, completeness, or usefulness of any information, apparatus, product, or process disclosed, or represent that its use would not infringe privately owned rights. Reference herein to any specific commercial product, process, or service by trade name, trademark, manufacturer, or otherwise, does not necessarily constitute or imply its endorsement, recommendation, or favoring by the United States Government, any agency thereof, or any of their contractors or subcontractors. The views and opinions expressed herein do not necessarily state or reflect those of the United States Government, any agency thereof, or any of their contractors.

Printed in the United States of America. This report has been reproduced directly from the best available copy.

Available to DOE and DOE contractors from
U.S. Department of Energy
Office of Scientific and Technical Information
P.O. Box 62
Oak Ridge, TN 37831

Telephone: (865) 576-8401
Facsimile: (865) 576-5728
E-Mail: reports@osti.gov
Online ordering: http://www.osti.gov/scitech

Available to the public from
U.S. Department of Commerce
National Technical Information Service
5301 Shawnee Rd
Alexandria, VA 22312

Telephone: (800) 553-6847
Facsimile: (703) 605-6900
E-Mail: orders@ntis.gov
Online order: https://classic.ntis.gov/help/order-methods/

SAND2018-1900
Printed February 2018
Unlimited Release

# Removal of Stationary Sinusoidal Noise from Random Vibration Signals

Brian K. Johnson, Jerome S. Cap
Environments Engineering & Integration
Sandia National Laboratories
P. O. Box 5800
Albuquerque, New Mexico 87185-MS0840

## Abstract

In random vibration environments, sinusoidal line noise may appear in the vibration signal and can affect analysis of the resulting data. We studied two methods which remove stationary sine tones from random noise: a matrix inversion algorithm and a chirp-z transform algorithm. In addition, we developed new methods to determine the frequency of the tonal noise. The results show that both of the removal methods can eliminate sine tones in prefabricated random vibration data when the sine-to-random ratio is at least 0.25. For smaller ratios down to 0.02 only the matrix inversion technique can remove the tones, but the metrics to evaluate its effectiveness also degrade. We also found that using fast Fourier transforms best identified the tonal noise, and determined that band-pass-filtering the signals prior to the process improved sine removal. When applied to actual vibration test data, the methods were not as effective at removing harmonic tones, which we believe to be a result of mixed-phase sinusoidal noise.

## ACKNOWLEDGMENTS

The authors would like to acknowledge Randall Mayes and Samuel Stearns for their work in developing the two noise removal methods discussed in this report (matrix inversion and chirp-z transform method, respectively).

## TABLE OF CONTENTS

## FIGURES

## TABLES



## NOMENCLATURE

| Abbreviation | Definition |
|---|---|
| **COV** | Coefficient of Variance |
| **CZT** | Chirp-Z Transform |
| **FFT** | Fast Fourier Transform |
| **PDF** | Probability Density Function |
| **PSD** | Power Spectral Density |
| **SOR** | Sine-on-Random |
| **SRR** | Sine-to-Random Ratio |

# 1. INTRODUCTION

The purpose of this document is to characterize two methods for identifying and removing sinusoidal waveforms from mixed sine-on-random (SOR) data. The fundamental techniques will be described along with their strengths and limitations. In addition to the two primary methods, additional techniques to improve their effectiveness will be discussed. Various examples will be given of both methods to demonstrate their strengths and weaknesses.

## 1.1. Outline

The following flowchart provides an overview of the process.

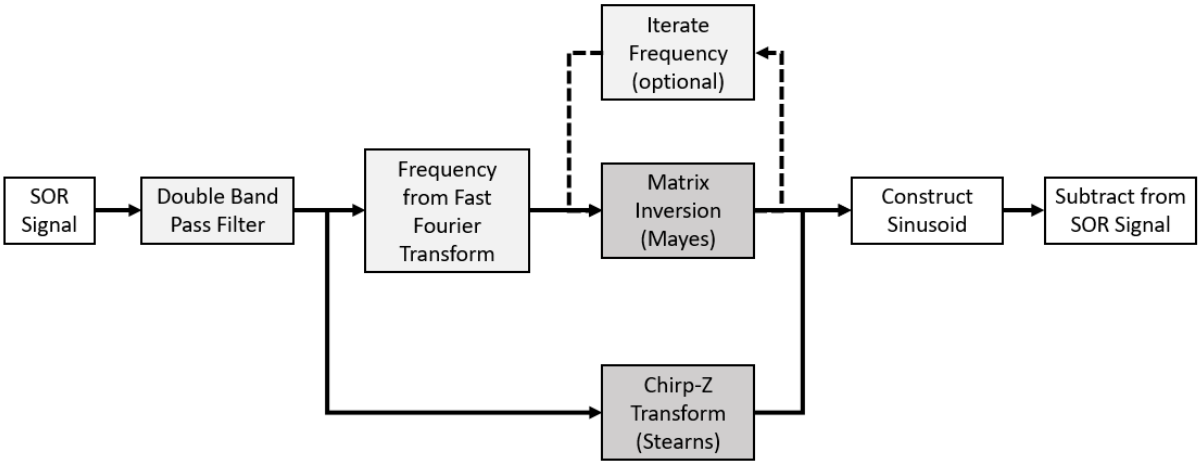


**Figure 1.** Sine removal process. The two primary methods (Mayes, Stearns) are darkly shaded. Additional techniques which we explored (filtering, Fourier transform frequency, iteration) are lightly shaded.

As shown in Figure 1, the original SOR signal is removed via one of two methods: a matrix inversion method developed by Randal Mayes or a chirp-z transform method by Samuel Stearns. This report will discuss these two methods as well as the additional techniques to increase their effectiveness, namely band pass filtering, fast Fourier transforms, and iteration (shown in Figure 1).

# 2. METHODS

The principle information required to remove sinusoidal content is the frequency, magnitude, and phase of the tone. Equation (1) shows the form of the noise that we wish to remove:

$$y = Asin(2\pi ft) + Bcos(2\pi ft) \quad (1)$$

where the sine amplitude $y$ is a function of time $t$ (in seconds), frequency $f$ (in Hz), and amplitudes $A$ and $B$. The unknown quantities that must be determined are $f$, $A$, and $B$. $A$ and $B$ characterize both the magnitude and phase of the tone. We examined two methods which determine the frequency, magnitude, and phase of the sinusoid: 1) Mayes' matrix inversion method and 2) Stearns' chirp-z transform method. The characteristics of the sinusoidal content must be time-invariant to achieve successful removal with the matrix inversion method. The chirp-z method can account for linear changes in frequency over time, but not changes in amplitude or phase.

Beyond an analysis of the primary sine removal methods, it is also necessary to discuss the pre- and post-processing techniques that we performed on the input signal. Pre-processing methods such as band pass filtering were implemented to enhance the chances for a successful tone extraction. We also used Rayleigh distribution analysis before and after sine removal to evaluate the characteristics of the signal and to determine the amount of sinusoidal content that was present.

MATLAB was the computational tool in which all methods were implemented.

## 2.1. Band Pass Filtering

A SOR signal may contain multiple tones, each with different frequencies. Attempting to remove all sinusoids at once with a single set of fitting functions will produce poor results, as each sinusoid takes on noise from all other sinusoids. In order to remove one tone at a time, it is necessary to band pass filter the SOR time history within as narrow of a frequency band as feasible bounding the tone in question. The filter attenuates the amplitude of any tones and random signal outside of that frequency band.

### *2.1.1. Filter Parameters*

We implemented a two stage filtering process. The first filter attenuates frequencies near to the pass band but has poor attenuation far from the pass band. Therefore, the second filter was introduced to attenuate frequencies far from the pass band.

The first filter is a second-order Chebyshev Type II filter. We chose this filter because of its sharper roll-off at the edge of the pass band, which greatly attenuates frequencies close to either side of the band. The pass band is 4 Hz, which is narrow enough to attenuate the majority of frequency content in the signal but is wide enough to account for variations in the frequency of the sine tone to be removed. Smaller bands also produced an uneven frequency response in the pass band. The attenuation

of the filter was set to 20 dB to similarly reduce as much signal content as possible outside the pass band while keeping the gain within the pass band close to 0. The filter runs from 0 Hz to the Nyquist frequency.

The second filter is a second-order Butterworth filter. A Butterworth was used because of its characteristic flat frequency response in the pass band. In addition, it has a higher attenuation farther from the pass band compared to the first filter (Chebyshev Type II). For similar reasons as the first filter, the pass band was set to 8 Hz and the attenuation to 60 dB to maximize the signal attenuation outside of the pass band while keeping the pass band gain at 0 dB. The filter runs from 0 Hz to the Nyquist frequency.

The frequency responses for both filters are shown in Figure 2 and Figure 3.

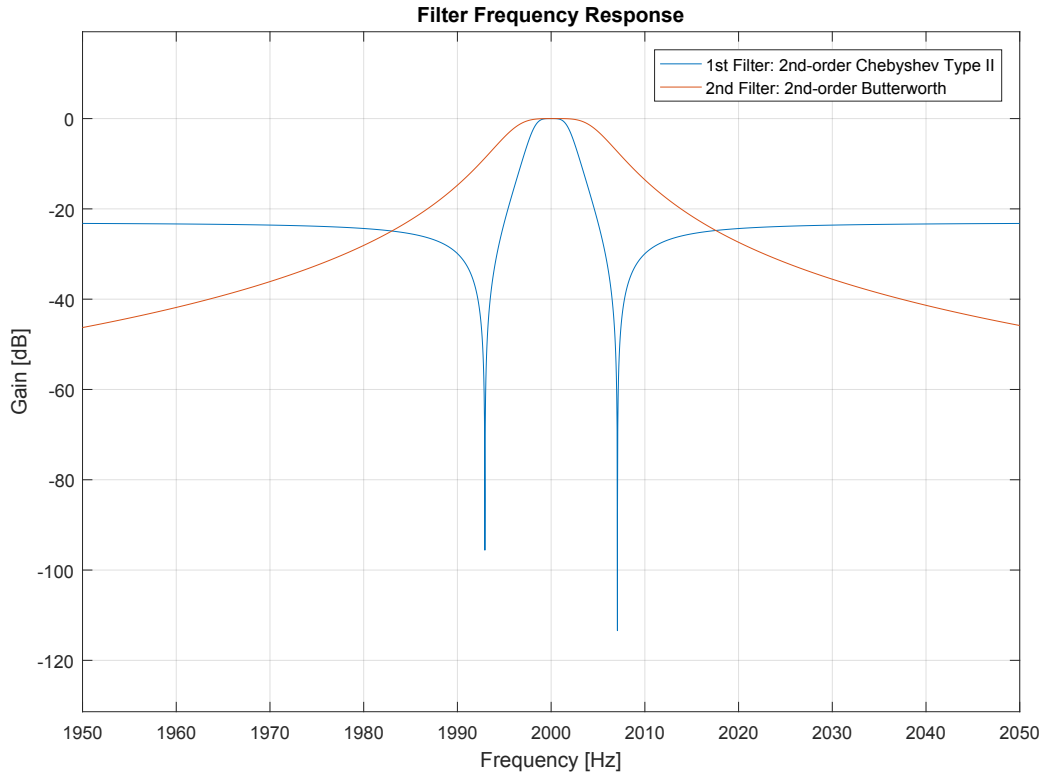


**Figure 2.** Filter frequency response in local frequency range.

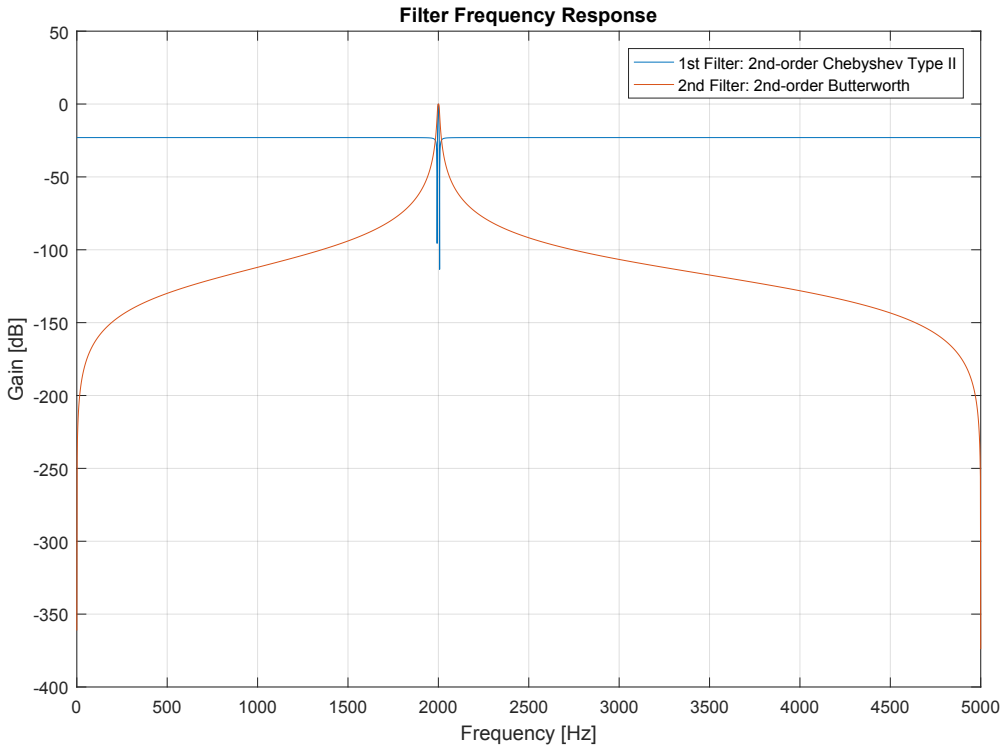


**Figure 3.** Filter frequency response in total frequency range (0 Hz to Nyquist).

The input signals are filtered in both the forward and reverse directions to eliminate any time delay in the filtered signal. This zero-phase digital filtering is necessary to preserve the original phase of the sinusoid being filtered.

### *2.1.2. Filter Transience and Removal*

After passing the signal through each band pass filter we observed a transient response in output amplitude during the first cycles of the signal. This is shown in Figure 4. A similar transient effect was also observed at the tail end of the signal.

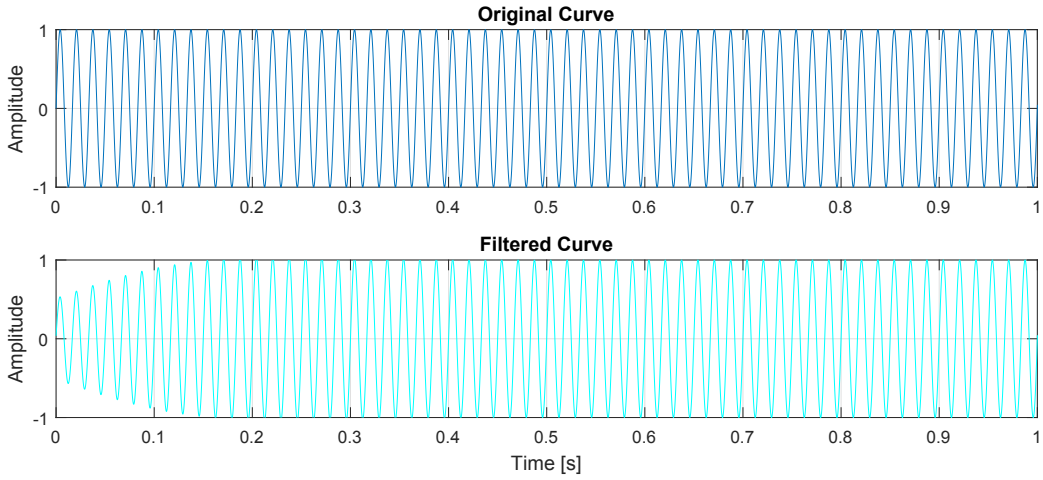


**Figure 4.** Transience after passing signal through band pass filter.

To improve the amplitude calculation from both sine removal methods we cropped the signal after the starting transience and before the ending transience. We created a formula to determine how many samples to remove, represented in Equation (2):

$$Tr = \frac{0.55 * length}{band^{0.89}} \tag{2}$$

where *Tr* is the number of transient samples, *length* is the number of samples of the filtered signal, and *band* is the frequency band of the band pass filter in Hz. The constants in Equation (2) were determined by an empirical study in which we recorded the length of transience for a variety of frequencies, filter bands, and sample rates and iterated the constants until they formed a fit with the data.

After cropping out the transient segments, the sine removal algorithm can be performed on the filtered signal. After a sine tone is fit to the signal using either removal method, we extended the tone back to the original start and end of the original uncropped signal so that the sine-removed output has no residual tonal content.

## 2.2. Verification of Sinusoidal Content

We applied statistical analysis as both a qualitative and quantitative measure of the presence of sinusoidal content the performance of the solver in removing it. The primary measure was the peak distribution of the band pass filtered signal. The distribution reveals information about the amount of sinusoidal versus random content present in the signal, and thus can be compared before and after applying the sinusoidal removal process to evaluate the results.

### *2.2.1. Rayleigh Distribution and Coefficient of Variance*

The probability density function (PDF) of the peak amplitudes of a stationary narrowband random signal follow a Rayleigh distribution. Pure sinusoidal stationary signals have a single amplitude and thus the PDF of the peaks has a single spike at that amplitude.

A useful quantitative metric associate with the peak distribution is the coefficient of variances (COV). It is defined by Equation (3).

$$COV = \frac{std}{mean} \tag{3}$$

where *std* and *mean* are the standard deviation and mean of the peaks respectively.

A Rayleigh distribution is characterized by a single parameter that relates both the mean and std. As a result, a signal for which the peaks follow a Rayleigh distribution will have COV = 0.5227. A pure stationary sinusoid will always have COV = 0

because the standard deviation of the peaks is zero. This information provides a quantitative metric which evaluates whether the signal is random, sinusoidal, or SOR.

A comparison of a narrowband random signal, a pure sinusoidal signal, and the combined SOR signal is shown in Figure 5. The COV of each of the examples is labeled in each plot.

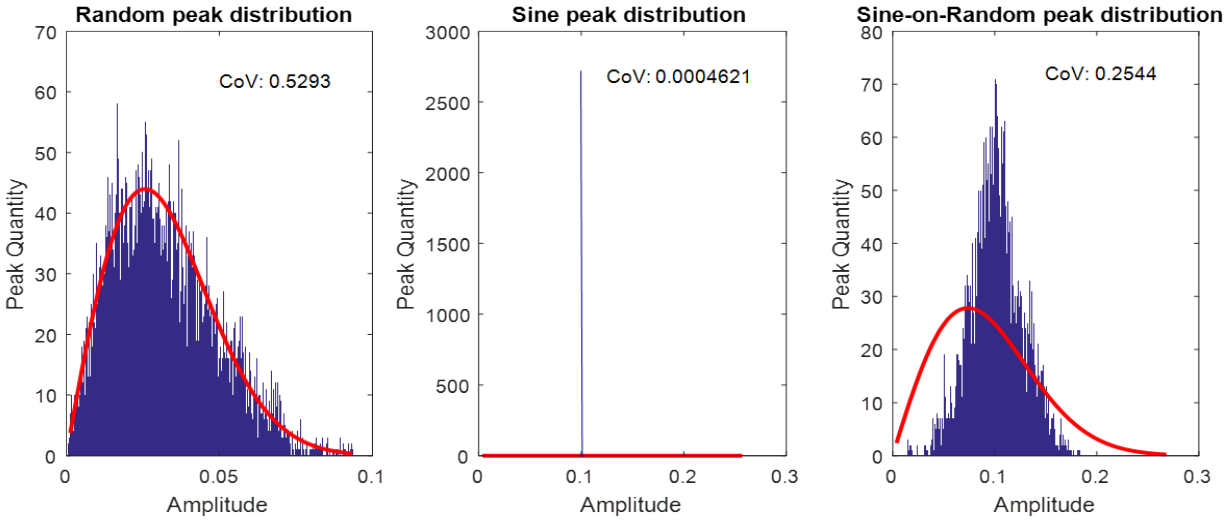


**Figure 5.** PDF for random, sine, and SOR signals with a Rayleigh fit (red).

The computed COV values match our expectations, as the random noise has a COV close to that of an ideal Rayleigh distribution, the sinusoid has a COV close to zero, and the SOR signal has a COV somewhere in between.

## 2.3. The Chirp-Z Transform Method

The first method of characterizing sinusoidal content that we examined was Sam Stearns' chirp-z transform (CZT) algorithm.

### *2.3.1. Chirp-Z Transform*

The CZT is a generalized discrete Fourier transform that effectively maps straight lines in the S-plane to spiral arcs on the Z-plane. Bluestein's Algorithm allows the CZT to be calculated by a set of fast Fourier transforms (FFTs). The general algorithm is shown in Equations (4) through (10) (Oppenheim and Schafer 1989).

$Convert\ N\ samples\ of\ the\ input\ signal,\ x_n$

$to\ M\ samples\ of\ the\ Z\ plane\ transform\ \ X_k$

$$L = N + M - 1 \tag{4}$$

$$y_n = \begin{cases} A^{-n} W^{n^2/2} x_n & n = 0, 1, 2, \ldots, N-1 \\ 0 & n = N, N+1, \ldots, L-1 \end{cases} \quad (5)$$

$$Y_r = \sum_{n=0}^{N-1} y_n e^{-\frac{i2\pi rn}{N}} \qquad r = 0, 1, \ldots, L-1 \quad (6)$$

$$v_n = \begin{cases} W^{-n^2/2} & 0 \le n \le M-1 \\ W^{-(L-n)^2/2} & L-N+1 \le n < L \\ arbitrary & all\ other\ n \end{cases} \quad (7)$$

$$V_r = \sum_{n=0}^{N-1} v_n e^{-\frac{i2\pi rn}{N}} \qquad r = 0, 1, \ldots, L-1 \quad (8)$$

$$g_k = \sum_{n=0}^{N-1} G_r e^{\frac{i2\pi rn}{N}} \qquad r = 0, 1, \ldots, L-1 \quad (9)$$

$$X_k = W^{k^2/2} g_k \qquad k = 0, 1, 2, \ldots, M-1 \quad (10)$$

### *2.3.2. Applying the Chirp-Z Transform*

Before applying the CZT, the signal is segmented and sent through a window function according to Stearns' algorithm. In general, we used two segments with a 50% overlap. The window function used in this study is a form of tapered cosine window, as shown in Figure 6. We examined several possible windows including Hann, Hamming, and Blackman windows, but the tapered cosine yielded the best results for the CZT.

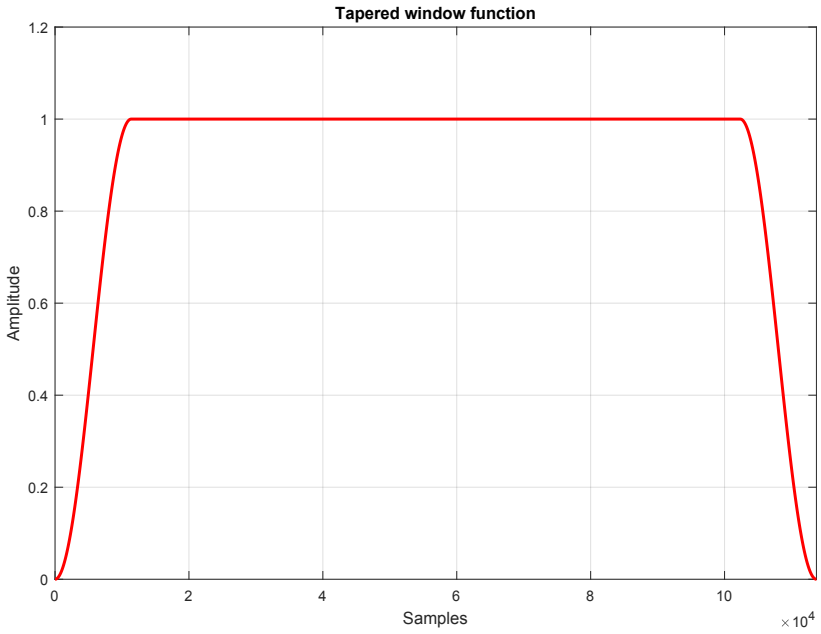


**Figure 6.** Tapered window function applied to signal.

The CZT is performed on each windowed signal with respect to an equally spaced range of frequencies, following the algorithm laid out in Section 2.3.1. Figure 7 shows the transform from the windowed signal to the Z plane (on real and imaginary axes).

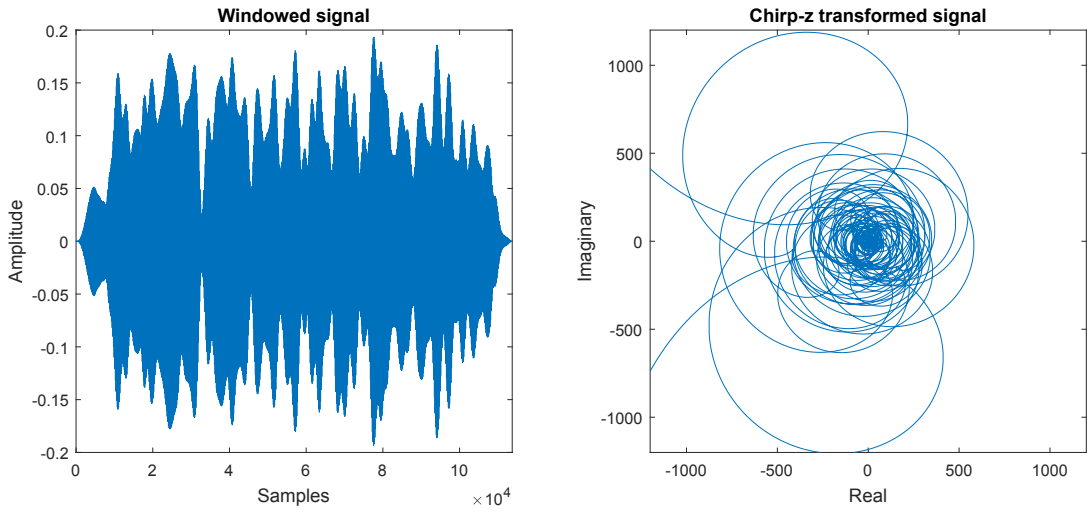


**Figure 7.** Signal in the time domain (left) and the Z-plane (right).

The transformed signals are turned into periodograms which estimate the power of the signal as a function of frequency, as shown in Figure 8. The peak power corresponds to the peaks of the periodograms. The periodograms use discrete samples, which affects the precision of the peak values. For this report, 1 million samples were used to provide a frequency resolution of 1e-9 Hz.

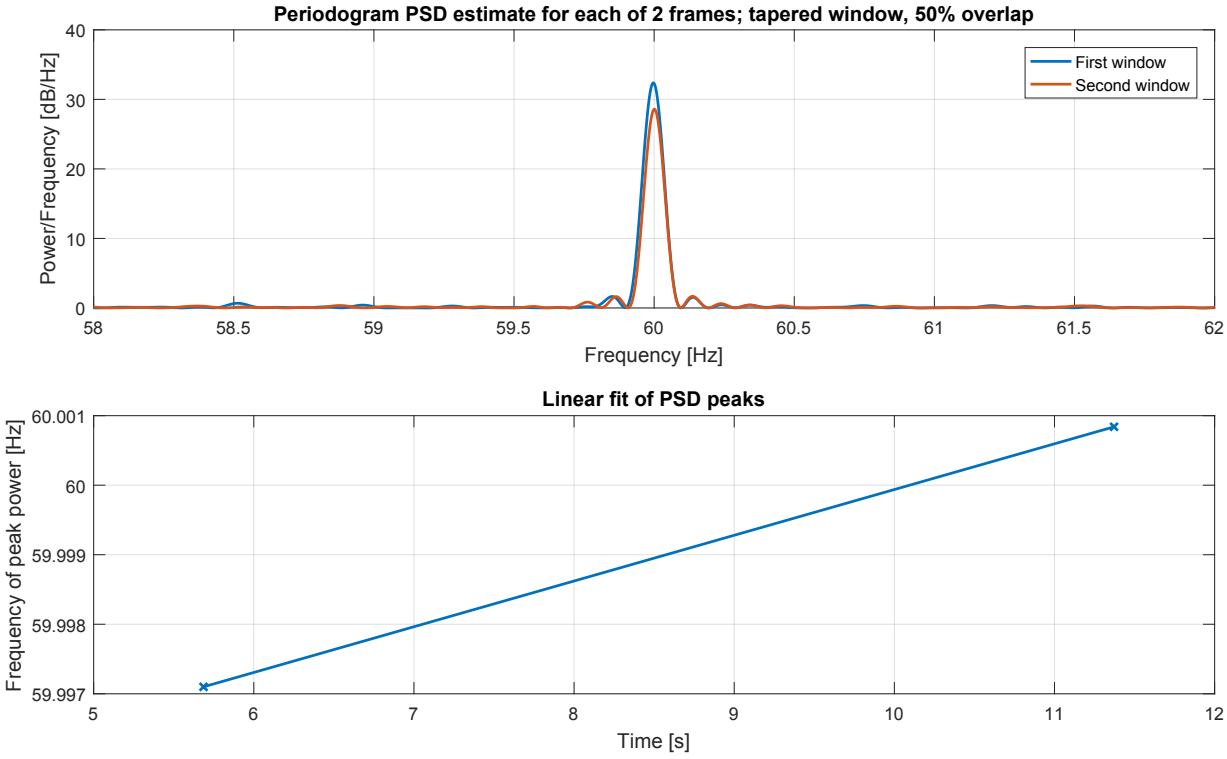


**Figure 8.** Periodograms from two tapered windows and the resulting linear fit.

The frequencies corresponding to the peak power are linearly fit, as shown in the bottom half of Figure 8. The linear fit has the form of Equation (11).

$$v(t) = c_1 t + c_0 \tag{11}$$

The coefficients from the linear fit are used to determine the frequency $f$ and amplitudes $A$ and $B$ of the sine tone. The y-intercept coefficient $c_0$ is the initial frequency of the tone. The slope $c_1$ is half of the chirp rate and is represented by β. The sine coefficients $A$ and $B$ which characterize the tone's amplitude and phase are thus calculated using Equations (12) through (14).

$$A = \sum x \cdot \frac{\sin(\theta)}{\sum sin^2(\theta)} \tag{12}$$

$$B = \sum x \cdot \frac{\cos(\theta)}{\sum cos^2(\theta)} \tag{13}$$

$$\theta = 2\pi(f + \beta K)K \tag{14}$$

where $f$ is the frequency in Hz, β is half the chirp rate, $\boldsymbol{x}$ is the signal, and $\boldsymbol{K}$ is the index of $\boldsymbol{x}$. Note that the sinusoidal argument $\boldsymbol{\theta}$ contains both $f$ and β and thus

accounts for any linear change of frequency recorded in the linear fit. For a stationary sinusoid, the theoretical solution has a chirp rate of zero and thus $\beta = c_1 = 0$.

## 2.4. The Matrix Inversion Method

The second method of characterizing sinusoidal content that we examined was Randall Mayes' matrix inversion algorithm. This algorithm is extremely sensitive to the accuracy with which the tonal frequency is selected. Therefore, in addition to the bandpass filtering operation, a tonal frequency identification scheme was employed. This frequency is then input into the algorithm which uses a Moore-Penrose pseudoinverse to find the *A* and *B* coefficients of the sine tone.

### *2.4.1. Frequency Determination with Fast Fourier Transforms*

After we band pass filter the signal using the filters described in 2.1.1, only the frequency content within the band of the filter should remain at an un-attenuated amplitude. Taking the FFT of this filtered signal shows the distribution of frequencies. Any sinusoidal content will appear on a plot of the FFT as a narrow spike with a large peak-to-valley ratio, centered at approximately the same frequency as the sine tone. The best estimate of the tonal frequency is the weighted average of the FFT peak and the adjacent points as described by Equation (15):

$$f_{est} = \frac{P_{n-1}f_{n-1} + P_n f_n + P_{n+1}f_{n+1}}{P_{n-1} + P_n + P_{n+1}} \tag{15}$$

where *n* is the index of the peak frequency, *f* is the frequency at a given index, and *P* is the amplitude at a given index. An empirical study to verify the accuracy of this equation is discussed in the Appendix. An example FFT is shown in Figure 9, where the points used in the weighted average are circled red. The resulting frequency estimate $f_{est}$ is the input to the matrix inversion method.

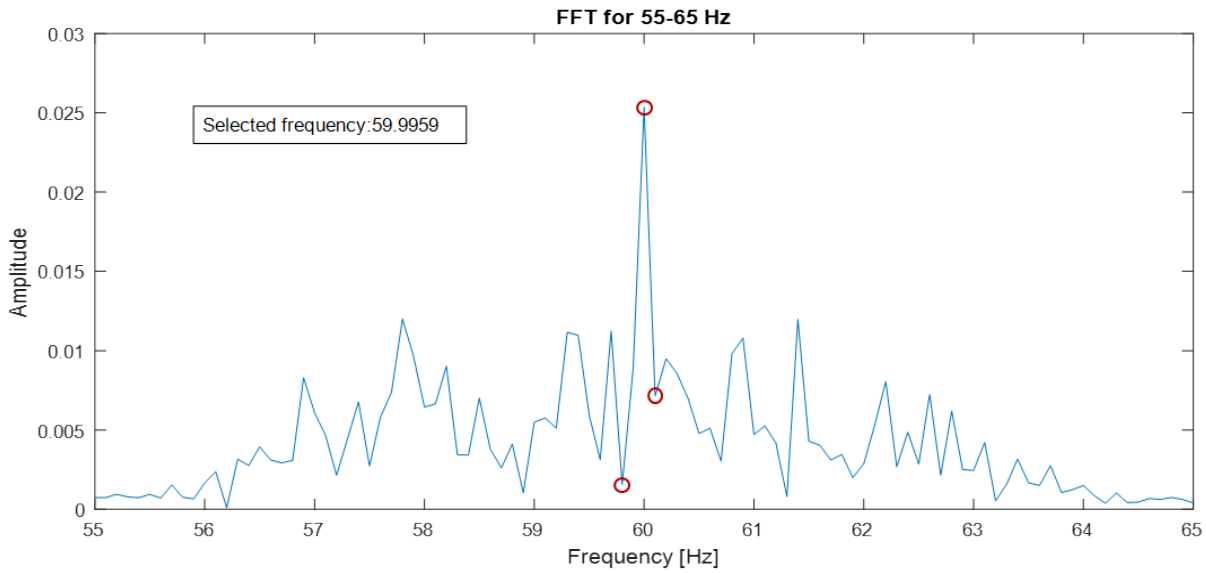


**Figure 9.** FFT of the band pass filtered signal. The three data points used to estimate the frequency are circled in red.

### *2.4.2. Matrix Inversion Algorithm*

The matrix inversion process uses the FFT frequency estimate from Equation (15) to obtain the A and B coefficients, thus fully characterizing the sinusoid. The algorithm is described in Equations (16) through (21):

| | Matrix size | |
|---|---|---|
| $X = \sin(2\pi f t)$ | $n - by - 1$ | (16) |
| $Y = \cos(2\pi f t)$ | $n - by - 1$ | (17) |
| $M = [X\ Y]$ | $n - by - 2$ | (18) |
| $M^I = pinv(M)$ | $2 - by - n$ | (19) |
| $C = M^I * x$ | $2 - by - n\ *\ n - by - 1$ | (20) |
| $[A\ B] = C$ | $2 - by - 1$ | (21) |

where $f$ is the input frequency in Hz, $\boldsymbol{t}$ is the time vector in seconds, $\boldsymbol{x}$ is the signal vector, and $A$ and $B$ are the output coefficients. However, based on the FFT frequency step size and the noise amplitude, the frequency estimate that is used in the matrix inversion process is not always accurate. To increase the accuracy of this estimate, we also adopted an iterative approach based on the initial FFT 'estimate' of the tonal frequency described in Section 2.4.1.

### 2.4.3. *Iterative Frequency Determination*

When the sine-to-random ratio (SRR) of a signal is very small, the FFT method of identifying the tonal frequency becomes less accurate. The goal of iterative frequency determination is to choose the frequency that best optimizes a given metric. For this study we used a examined all of the frequencies in a 2 Hz band centered on the initial FFT tonal frequency using a small incremental frequency step. The step size was determined by the minimum required resolution, which we discuss in Section 2.4.4.

There are two primary metrics to determine which frequency is the best choice for the tonal frequency. The first metric is the magnitude of the resulting sine tone. This follows the concept that the most complete removal of the sine tone corresponds to the sine tone with the largest possible amplitude. We calculated the amplitude $P_{sine}$ using Equation (22):

$$P_{sine} = \sqrt{A^2 + B^2} \tag{22}$$

where $A$ and $B$ are the amplitude coefficients from the matrix inversion results. The variation of sine amplitude as a function of the input frequency for the matrix inversion is plotted for example data in Figure 10. Note that the global maximum of the sine amplitude is near the true frequency of the tone, 60 Hz, but is not in perfect alignment.

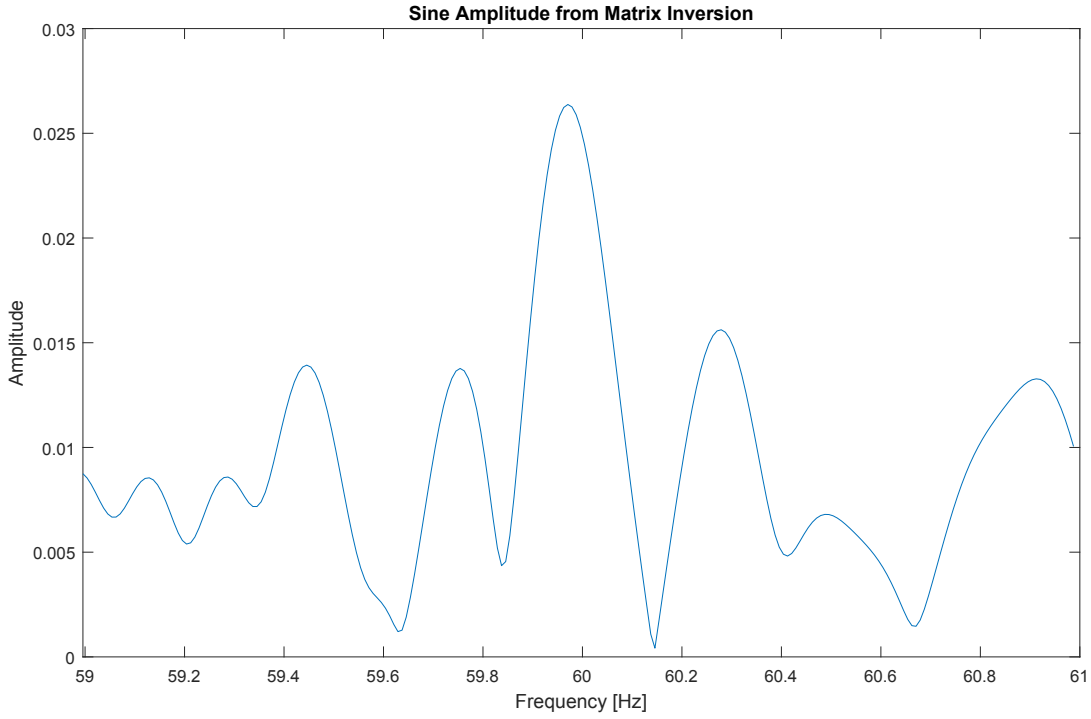


**Figure 10.** Optimization for amplitude of the removed sine tone. The x-axis shows the frequency that was input to the matrix inversion, and the y-axis is the resulting sine amplitude for each corresponding input frequency.

The second metric uses the RMS of the power spectral density (PSD) in the narrow band of frequencies near the input frequency. For each step in frequency in the 2 Hz band, a PSD of the sine-removed signal is created and the RMS is calculated from the same frequency band. The RMS corresponds to the area under the curve of the PSD plot so it is expected that the global minimum of RMS corresponds to the frequency that removes the most of the sine content. Using the same example data used to generate Figure 10, the effect of input frequency on the RMS is shown in Figure 11.

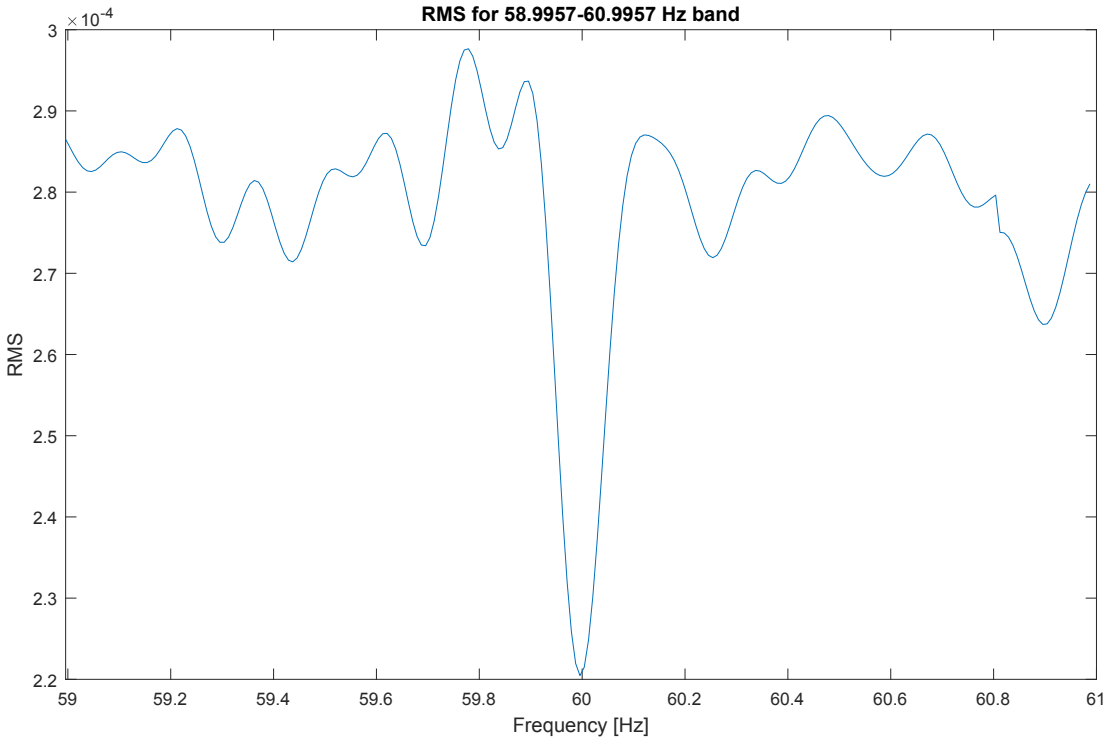


**Figure 11.** Optimization for RMS of the PSD curve. The x-axis shows the frequency that was input to the matrix inversion, and the y-axis is the resulting RMS of the signal corresponding to each input frequency.

As Figure 11 shows, the RMS is minimized at the frequency of the sine tone. Note that in comparison with the sine amplitude optimization, the RMS optimization tends to have a more accurate result. However, this is not always the case and the RMS metric is more computationally expensive to implement, thus the sine amplitude optimization remains useful.

A three dimensional plot of the PSD was created as shown in Figure 12. Note that the plane highlighted in red matches the profile of Figure 11 due to the relationship between RMS and the PSD curve. As the plot suggests, 60 Hz is the correct frequency of the tone because removing that frequency tone corresponds to the valley created in the PSD plot.

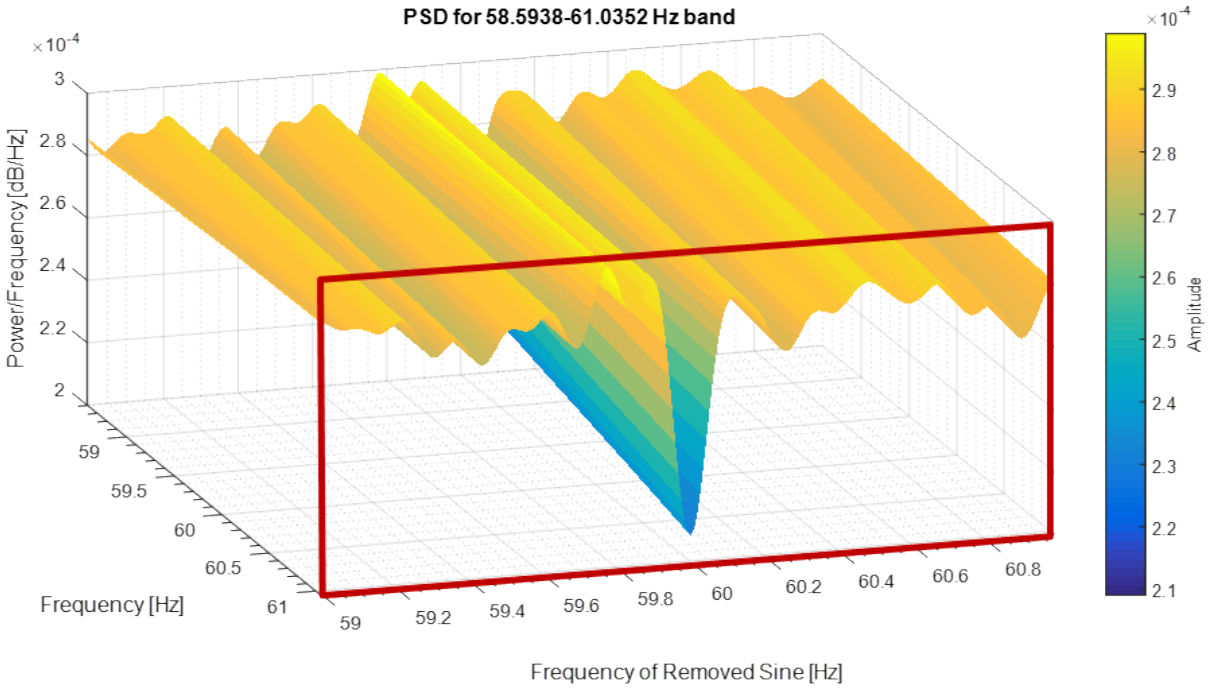


**Figure 12.** PSD vs. change in matrix inversion input frequency. The Frequency axis is the x-axis of the PSD in that frequency band. The Removed Sine Frequency axis is the frequency that is input to the matrix inversion method.

Examining the response of the FFT is also a useful metric to verify that the correct frequency was selected. When the frequency of the removed tone matches the actual frequency of the tone, the corresponding peak in the FFT should be eliminated. Figure 13 shows the response of the FFT plot as the removed frequency is varied in a 2 Hz band.

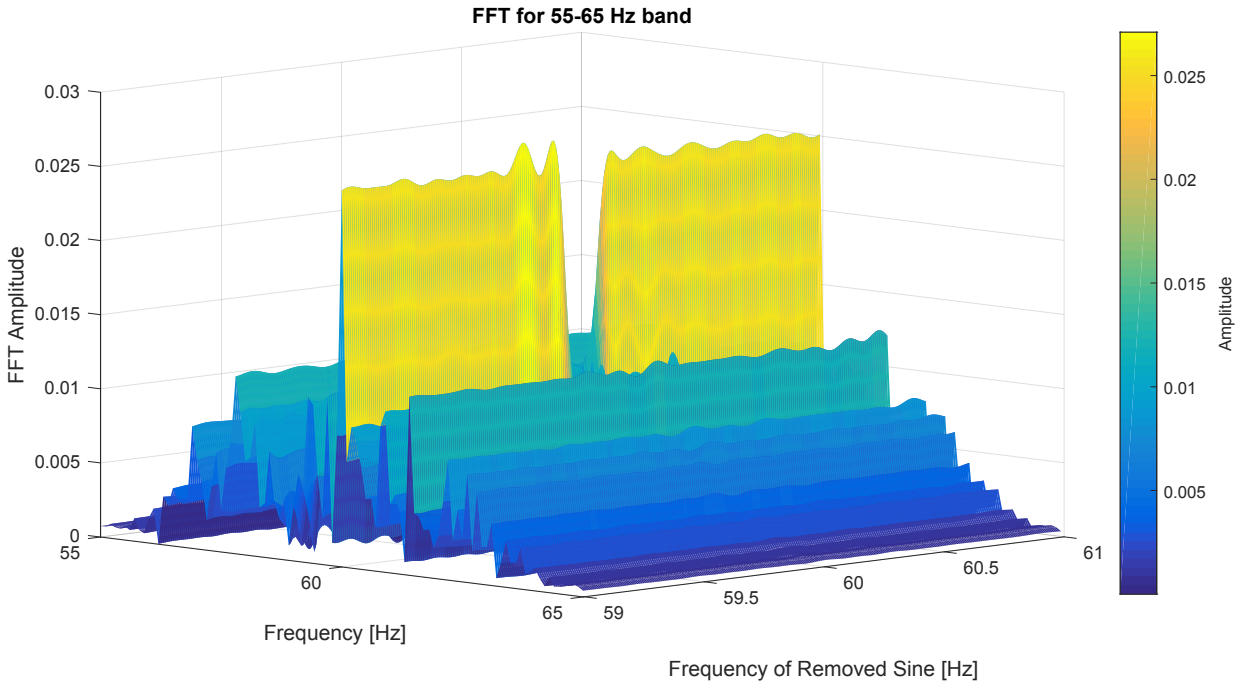


**Figure 13.** FFT vs. change in matrix inversion input frequency.

This is a helpful tool for verification but is not as accurate as the sine amplitude or RMS metrics because the FFT of the random portion of the signal can be unpredictable. The sine frequency that creates a valley in the FFT peak does not always correlate to the true sine frequency.

It must be noted that the iterative tool is only applicable to Mayes' matrix inversion method. Stearns' CZT method couples together the sine frequency and amplitude calculations so there is no way to iterate the frequency to create a more accurate amplitude.

### *2.4.4. Required Frequency Resolution*

Removing the incorrect frequency creates a beating effect as shown in Figure 14. In this example a 2.1 Hz tone of amplitude 1 was subtracted from a 2 Hz tone of the same amplitude. Over time the waveforms overlap and the total amplitude of the signal exceeds that of either individual tone. The dotted lines mark the threshold of amplification, when the amplitude is greater than 1.

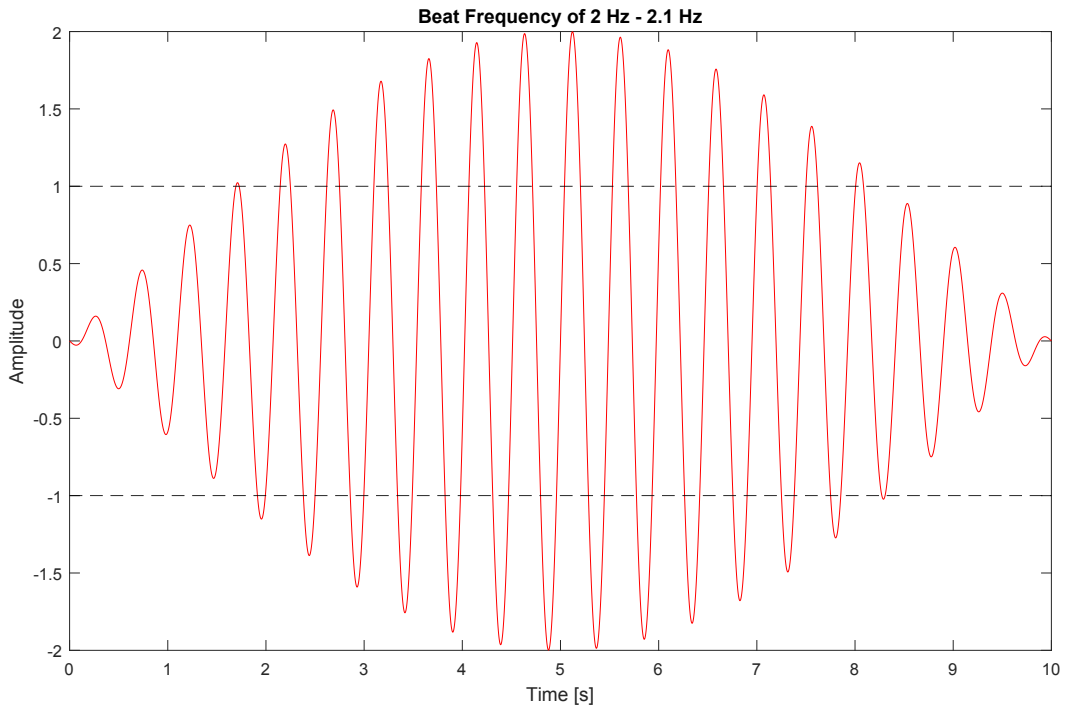


**Figure 14.** Beat frequency caused by removal of incorrect frequency tone. Dotted lines mark the threshold of amplification.

We found that amplification begins to occur soon after the estimated and true frequencies are approximately 1/6 of a wavelength apart in time. Because the frequency beats in time, the wavelength and period are equivalent. Equation (23) shows the relationship between time history length and frequency resolution:

$$L = \frac{\lambda}{6} = \frac{T}{6} = \frac{1}{6f_r} \tag{23}$$

where $L$ is the time history length in seconds, $\lambda$ is the true frequency wavelength in seconds, $T$ is the period in seconds, and $f_r$ is the beat frequency in Hz. This rearranges to the solution for the beat frequency shown in Equation (24):

$$f_r = \frac{1}{6L} \tag{24}$$

The beat frequency $f_r$ is equivalent to the maximum allowable difference between the true and estimated frequencies. Thus any frequency solution that deviates more than $f_r$ from the true frequency will result in ineffective removal of sine tone and potential sine amplification of the sine for time histories of length $L$ or longer.

# 3. TEST CASES

We used three test cases to evaluate the effectiveness of both the matrix inversion and chirp-z methods, as well as the supplemental techniques discussed (band pass filtering, iterative frequency solving, and COV analysis). Our first two cases use theoretical, fabricated SOR signals, of which the first case is simple and straightforward and the second case is more difficult to analyze. The third case uses actual random vibration test data.

## 3.1. Test Case 1: Fabricated SOR with High SRR

The first test case is a fabricated SOR signal with a high SRR. The signal follows the format described in Table 1. The signal is composed of three sine tone components added to a random component. We used the MATLAB function *randn* to create the random component.

**Table 1.** Fabricated SOR #1 Characteristics.

| **Signal Characteristics** | | |
|---|---|---|
| Sample Rate [sample/s] | 10,000 | |
| Signal Length [s] | 100 | |
| Number of samples | $10^6$ | |
| Random signal RMS | 1 | |
| **Sine Tone Characteristics** | | |
| Frequency [Hz] | Amplitude | Phase, relative to t = 0 [rad] |
| 60 | 10 | 0 |
| 180 | 5 | 0 |
| 600 | 1 | 0 |

A segment of the time history is shown in Figure 15. A PSD of the signal is shown in Figure 16. Note the easily distinguished peaks in power at 60, 180, and 600 Hz compared to the random signal floor.

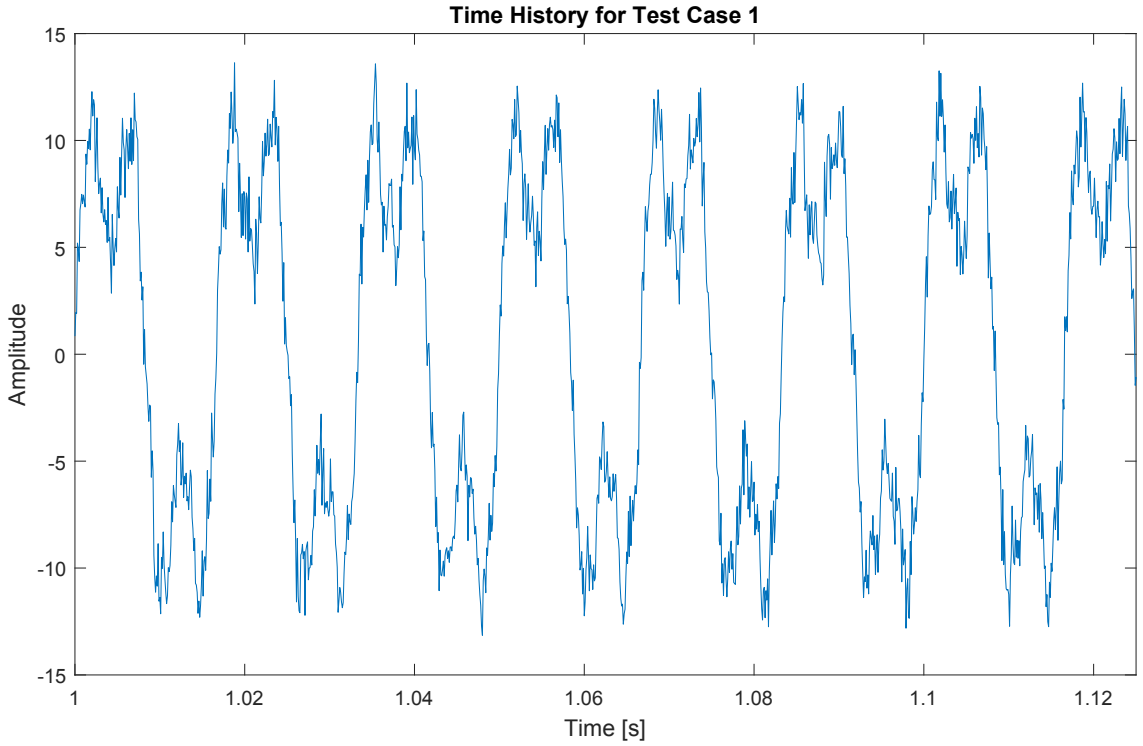


**Figure 15.** Time history segment of Test Case 1.

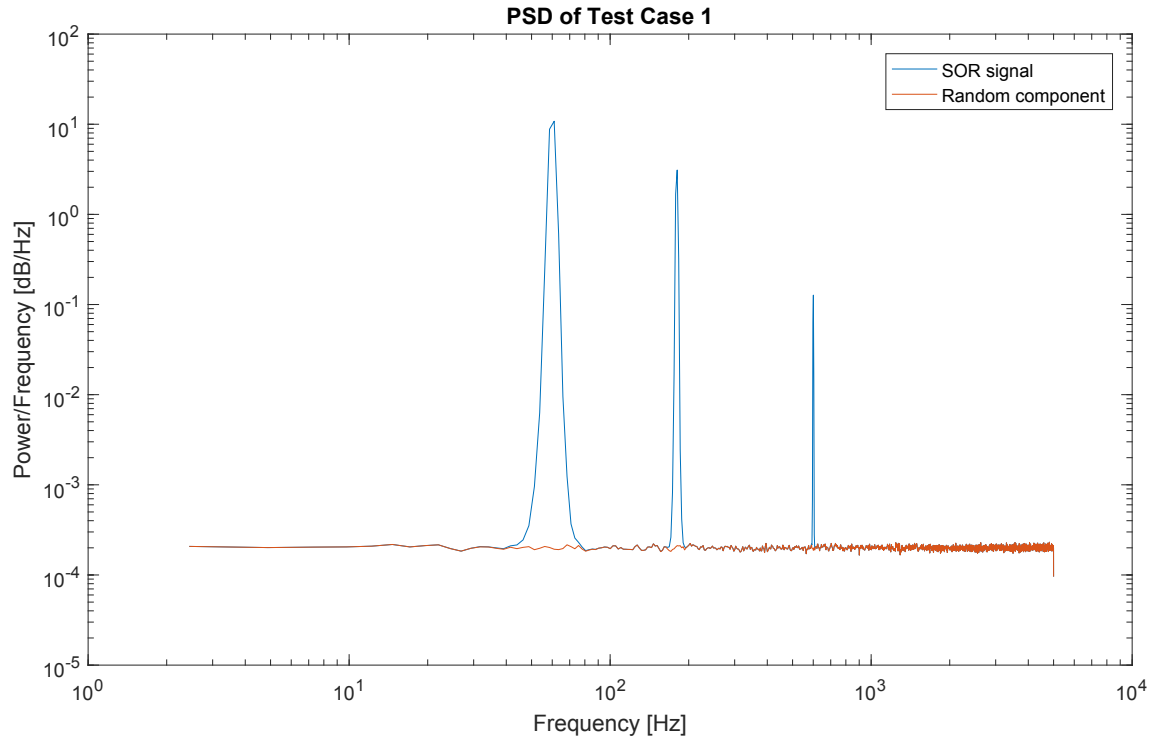


**Figure 16.** PSD of Test Case 1.

## 3.2. Test Case 2: Fabricated SOR with Low SRR, Phase Shifts

The second test case is a fabricated SOR signal with a lower SRR and follows the format described in Table 2, similar to Test Case 1. Compared to Test Case 1, the frequencies of the tones are the same, but the amplitudes of Test Case 2 are much smaller and two of the three tones have phase shifts added. Also note that the signal length is shorter, resulting in a fewer number of samples to analyze.

**Table 2.** Fabricated SOR #2 Characteristics.

| **Signal Characteristics** | | |
|---|---|---|
| Sample Rate [sample/s] | 10,000 | |
| Signal Length [s] | 5 | |
| Number of samples | 50,000 | |
| Random signal RMS | 1 | |
| **Sine Tone Characteristics** | | |
| Frequency [Hz] | Amplitude | Phase, relative to t = 0 [rad] |
| 60 | 0.25 | 0 |
| 180 | 0.02 | $\pi/3$ |
| 600 | 0.01 | $\pi/5$ |

A segment of the time history is shown in Figure 17 and a PSD is shown in Figure 18. Note that although the 60 Hz tone is still well visible in the PSD plot, the 180 Hz and 600 Hz tones are almost impossible to distinguish from the random signal floor.

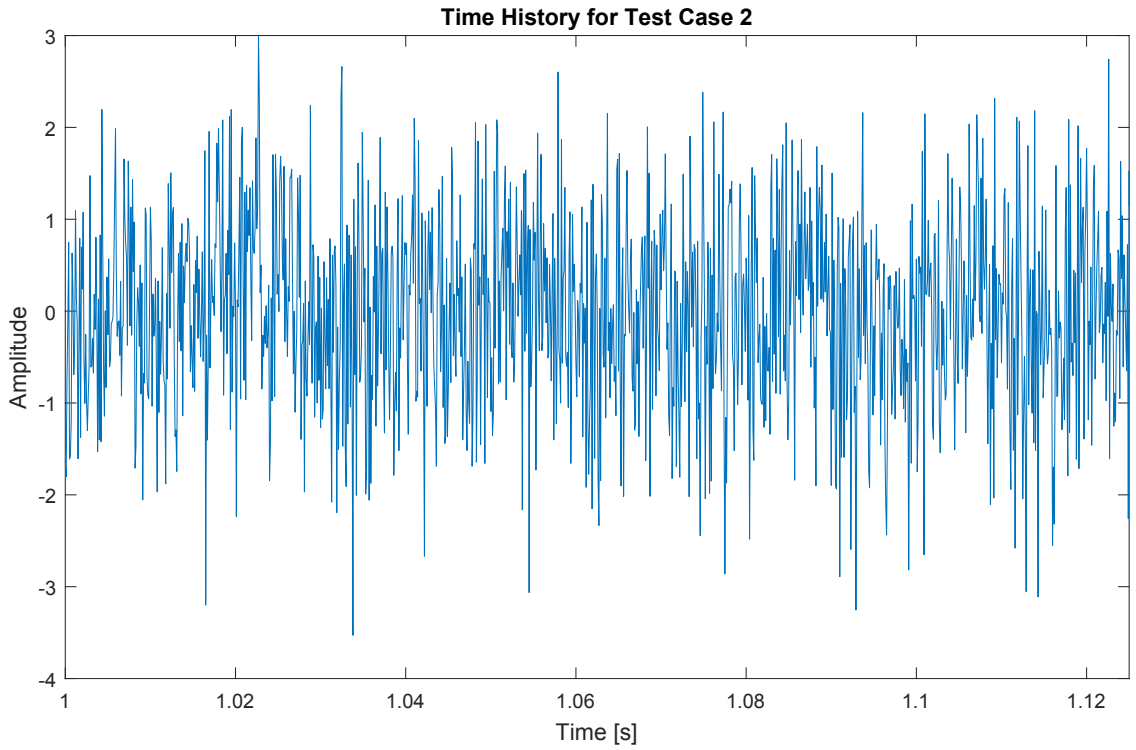


**Figure 17.** Time history segment of Test Case 2.

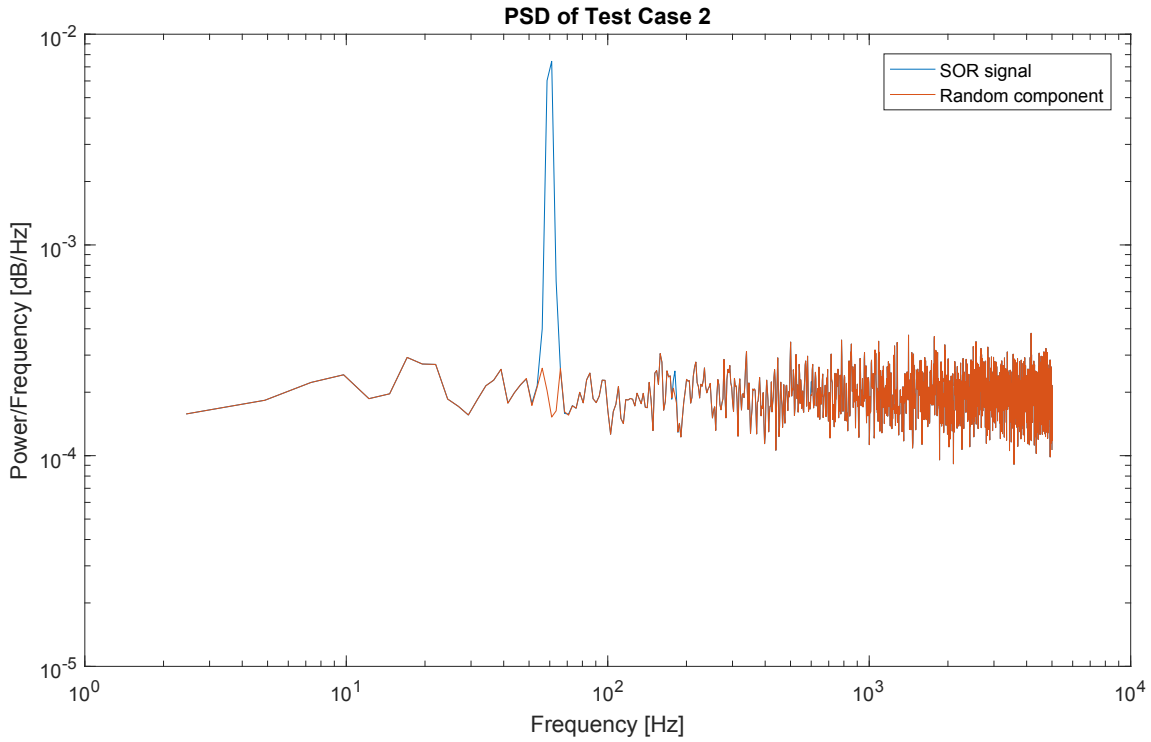


**Figure 18.** PSD of Test Case 2.

## 3.3. Test Case 3: Real Vibration Test Data

The third and final test case uses actual data from a random vibration test. Information about the signal is tabulated in Table 3. Figure 19 and Figure 20 respectively show the time history and PSD of the data. Because 60 Hz harmonic line noise is suspected in this data, the frequencies to be analyzed are 60 Hz, 180 Hz, 300 Hz, and 420 Hz which all correspond to significant peaks in the PSD.

**Table 3.** Vibration Data Characteristics.

| **Signal Characteristics** | |
|---|---|
| Sample Rate [sample/s] | 12,800 |
| Signal Length [s] | 62.72 |
| Number of samples | 802,816 |

The signal time history is shown in Figure 19 and a PSD is shown in Figure 20. The PSD plot shows pronounced peaks at 60 Hz and its odd harmonics of 180, 300, and 420 Hz. This is suggestive of electrical line noise which should be removed from the signal to obtain the true vibration response.

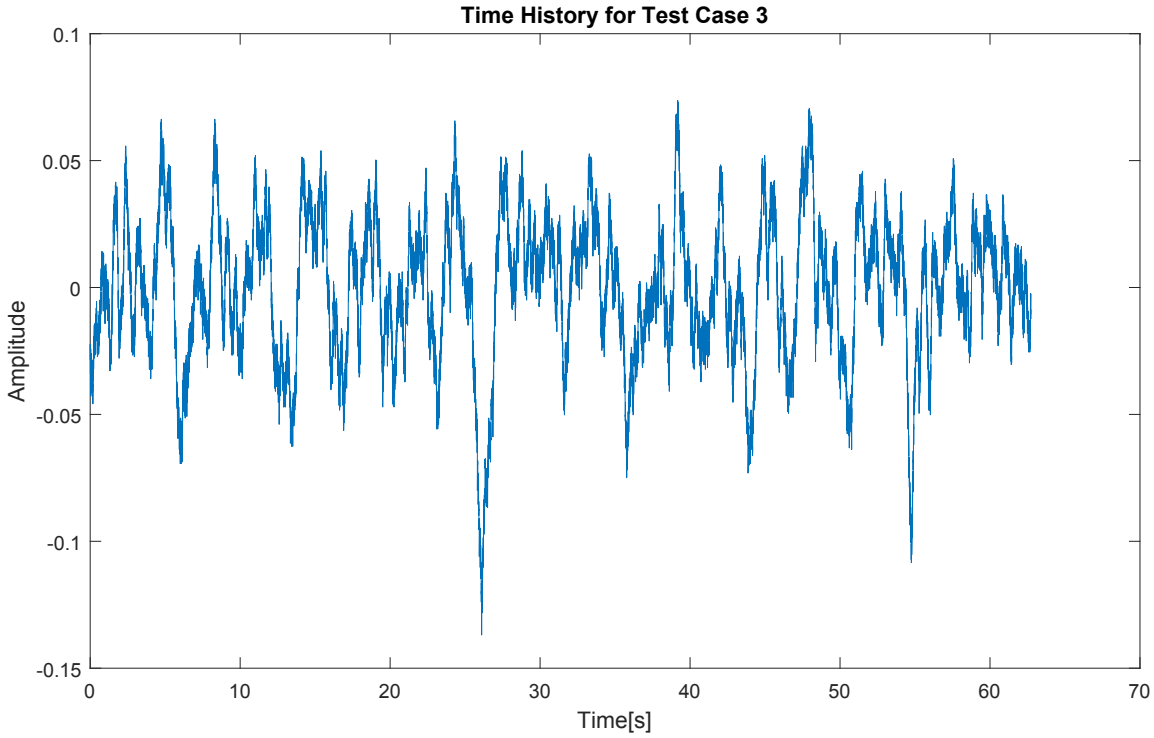


**Figure 19.** Time history segment of Test Case 3.

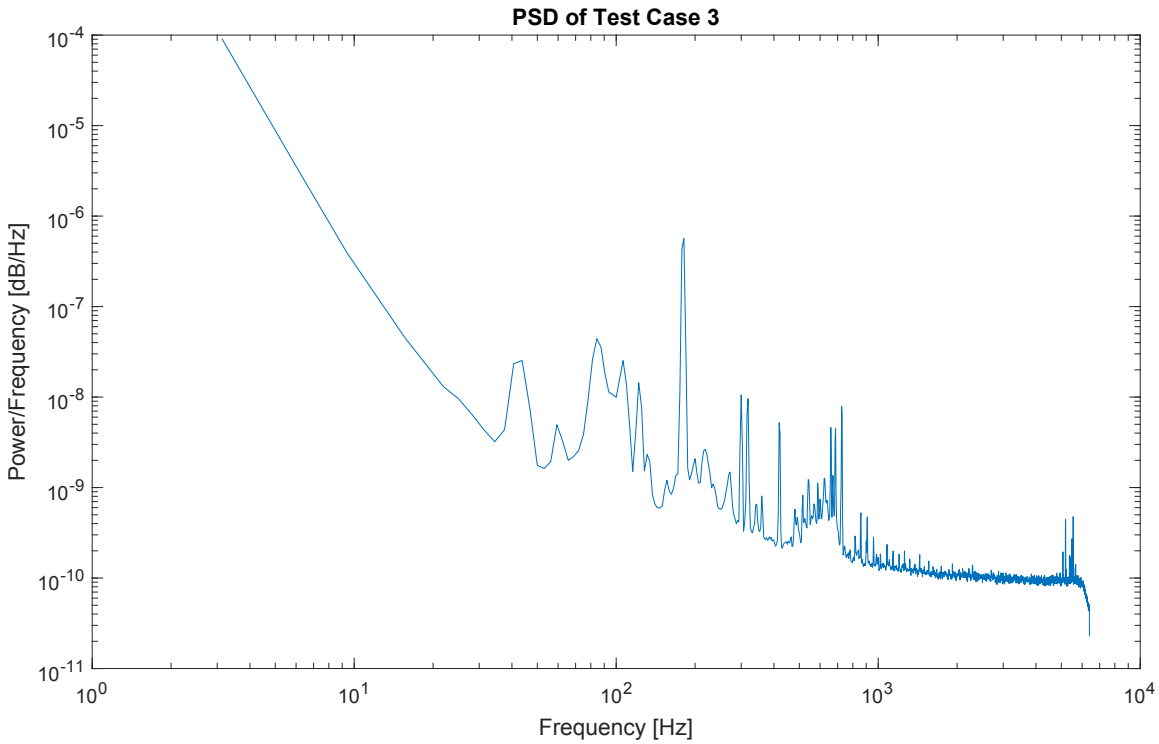


**Figure 20.** PSD of Test Case 3.

# 4. RESULTS OF ANALYSIS

The results of both sine removal methods on the three test cases are described below.

## 4.1. Summary of Results

For high SRR, the matrix inversion and chirp-z methods performed nearly identically, but chirp-z performed best. Both were able to remove the high amplitude sine tones. Iterative methods were not necessary because the initial frequency estimate derived from the FFT was already within the required resolution of accuracy. The COV metric was an accurate measure of tonal content before and after removal. It is proven that band pass filtering the signals improves sine removal results.

For low SRR, the matrix inversion method performed best. The chirp-z technique was unable to remove tones with very low SRR. However, the matrix inversion removed additional random content which we want to keep and not just the sine tone. Iterative methods identified the frequencies that removed the most content, but did not identify the exact frequency of each sine tone. The COV metric was not useful at low SRR and there was no observable correlation between COV and amount of tonal content at this SRR.

For the real test data, the 60 Hz tone was successfully removed by both methods. For all other tones, the matrix inversion method performed best, but neither method was able to remove all of the tonal content. The COVs and PDFs suggested that most of the content was removed, but the peaks in the PSD remained. One potential explanation may be that the higher frequency tones were multi-phased rather than a single sine form. Another explanation is that several tones with similar but not equal frequencies are clustered at the 60 Hz harmonics as suggested by the FFT of the signal.

## 4.2. Results: Test Case 1 (High SRR)

Both removal methods (matrix inversion, CTZ) were applied to Test Case 1. Band pass filtering was used in each case. The FFT tool was used for the matrix inversion method. The iteration tool was not used with the matrix inversion solver because the FFT tool produced a near perfectly accurate frequency solution. A subcase in which band pass filtering was not used is described in Section 4.2.1.

The comparison of the PSD before and after removal is shown in Figure 21. The PSD for the random signal is also plotted to provide a comparison against the sine-removed signal. A magnified view of the remaining sinusoidal content is shown in Figure 22.

The chirp-z method removed almost all sinusoidal content and the resulting PSD overlaps the random signal floor. Although the matrix inversion method removed the majority of sinusoidal content, a small portion remains. The signal was not impacted at any other frequencies besides those selected.

A parametric synopsis of the results are tabulated in Table 4.

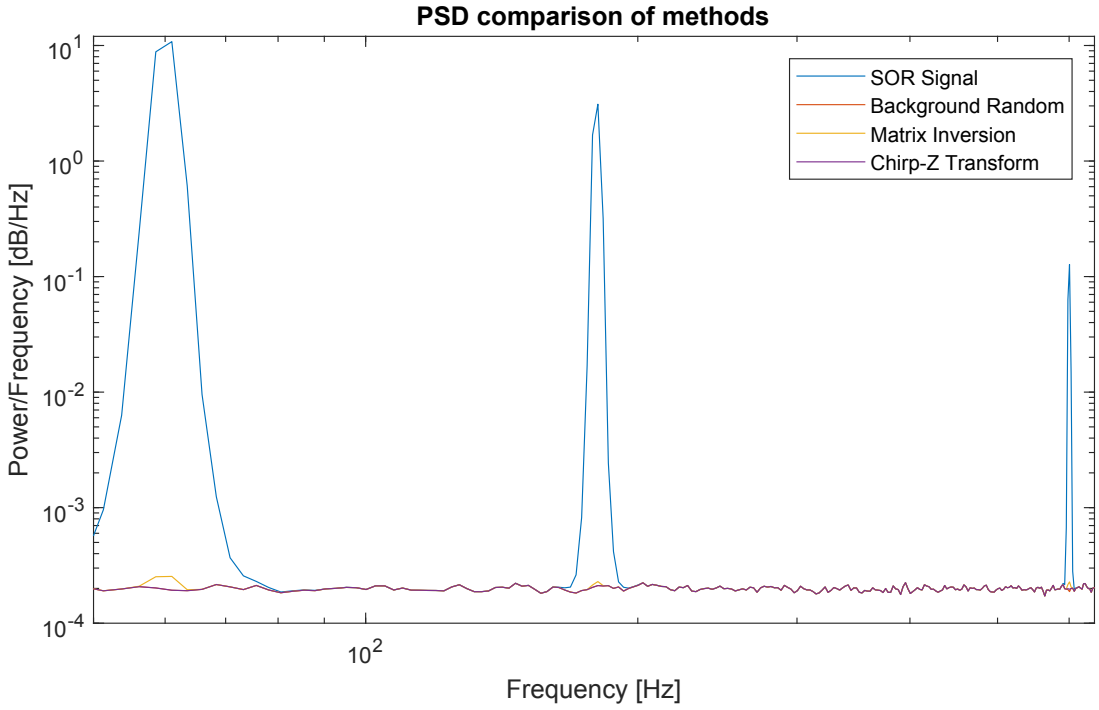


**Figure 21.** Case 1 PSD before and after applying matrix inversion removal.

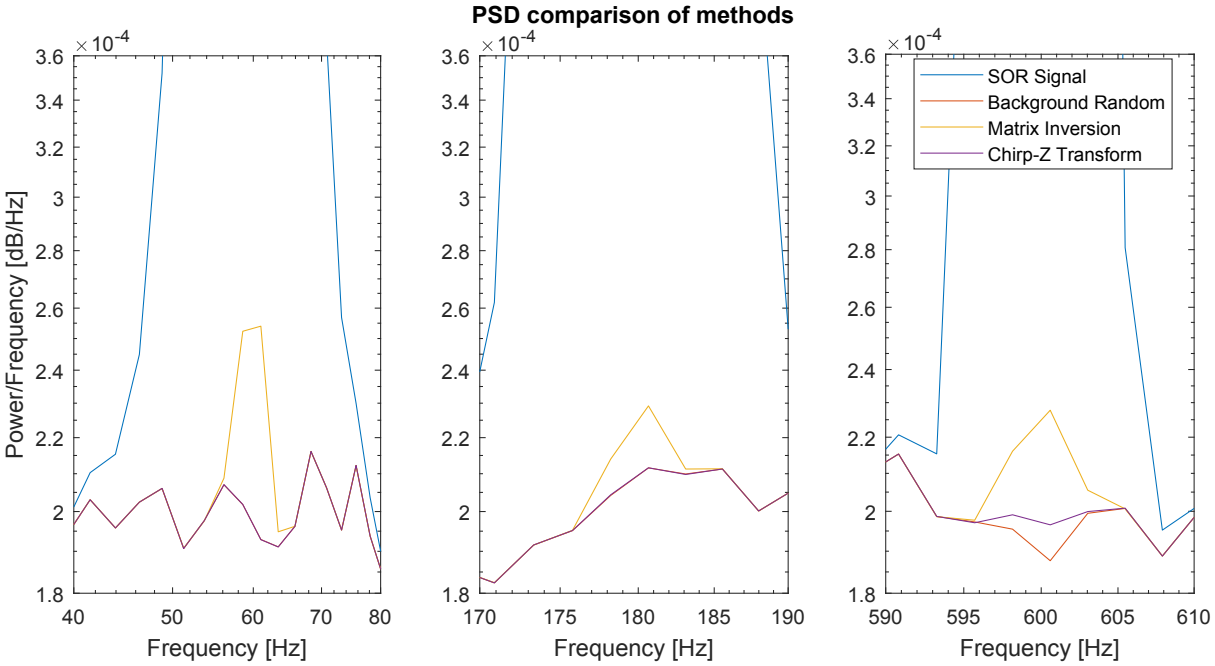


**Figure 22.** Case 1 magnified view of remaining sine tones.

**Table 4.** Case 1 results.

| | Tone | Actual | Matrix | Chirp |
|---|---|---|---|---|
| **Frequency (Hz)** | 1 | 60 | 60 | 60 |
| | 2 | 180 | 180 | 180 |
| | 3 | 600 | 600.0001 | 600 |
| **Amplitude** | 1 | 10 | 9.9874 | 9.9990 |
| | 2 | 5 | 5.004 | 5.0001 |
| | 3 | 1 | 1.0013 | 1.0014 |
| | | | | |
| **COV** | **Tone** | **Before** | **After (Matrix)** | **After (Chirp)** |
| | 1 | 0.00337 | 0.514 | 0.475 |
| | 2 | 0.00712 | 0.542 | 0.522 |
| | 3 | 0.0255 | 0.525 | 0.548 |

The FFT method obtained a very accurate value for the tonal frequency. The CZT method of obtaining frequency was exactly correct for all frequencies.

The matrix inversion method was not as accurate in its amplitude calculations as the chirp-z method, which may explain the inability to completely remove the tones.

The COV values provide quantitative verification that the initial signals were sine tones because the COV values before removal were very close to 0. After the tones were removed, the new COV values were close to the Rayleigh distribution value of 0.5227 which matches random noise. This verifies that the initial signals were sinusoids, and that the resulting signals were random.

### *4.2.1. Case 1 Bandpass Filter Study*

A second study was performed to examine the effectiveness of the dual band pass filter technique described in 2.1. For this study the signal were not bandpass filtered prior to applying the tone removal algorithms. The results are plotted in Figure 23. Comparing these results against those in Figure 21 clearly shows the value of employing the bandpass filtering technique.

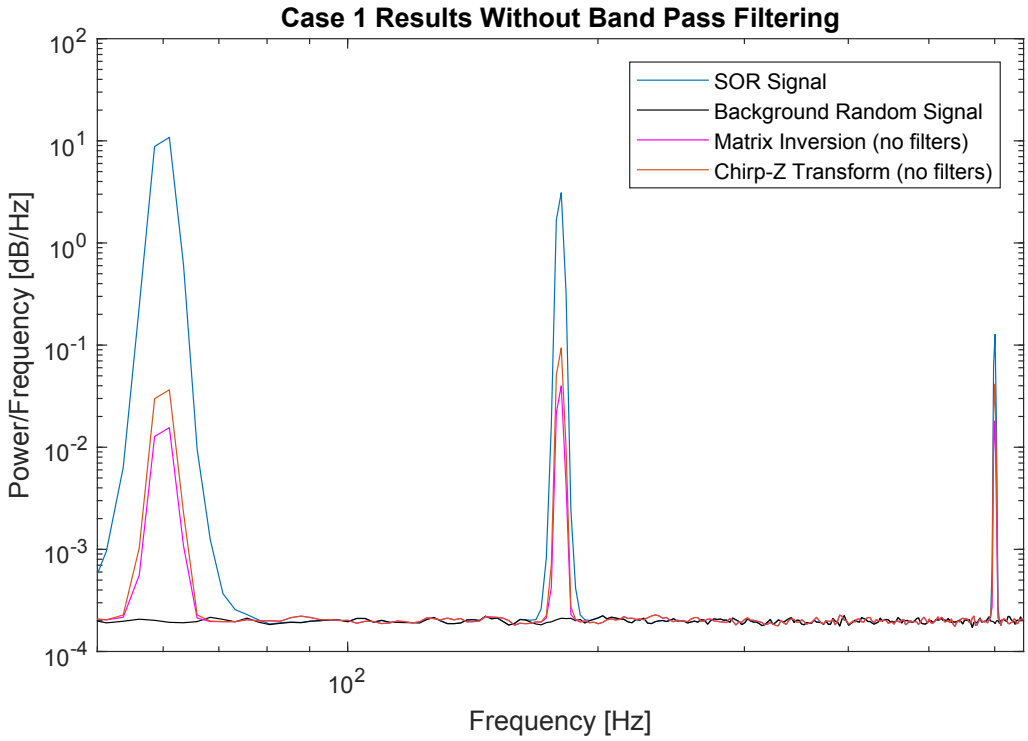


**Figure 23.** Case 1 comparison of results with and without band pass filtering.

As the plot shows, passing the signal through the band pass filters significantly improved the ability to remove the sine tones. The amount of remaining tonal content decreased by several orders of magnitude for both methods.

## 4.3. Results: Test Case 2 (Low SRR)

Both removal methods (matrix inversion, CTZ) were applied to Test Case 2. Band pass filtering was used in each case. The FFT tool was used for the matrix inversion method. The iteration tool was not used in the main results, but was applied to the matrix inversion solver in a subcase described in Section 4.3.1.

The comparison of the PSD before and after removal is shown in Figure 24. The PSD for the random signal is also plotted to provide a comparison against the sine-removed signal. A magnified view of the remaining sinusoidal content is shown in Figure 25.

A parametric synopsis of the results are tabulated in Table 5.

Figure 24 shows that while both methods removed the tone at 60 Hz, the chirp-z method did slightly better. However, only the matrix inversion method removed the tones at 180 Hz and 600 Hz.

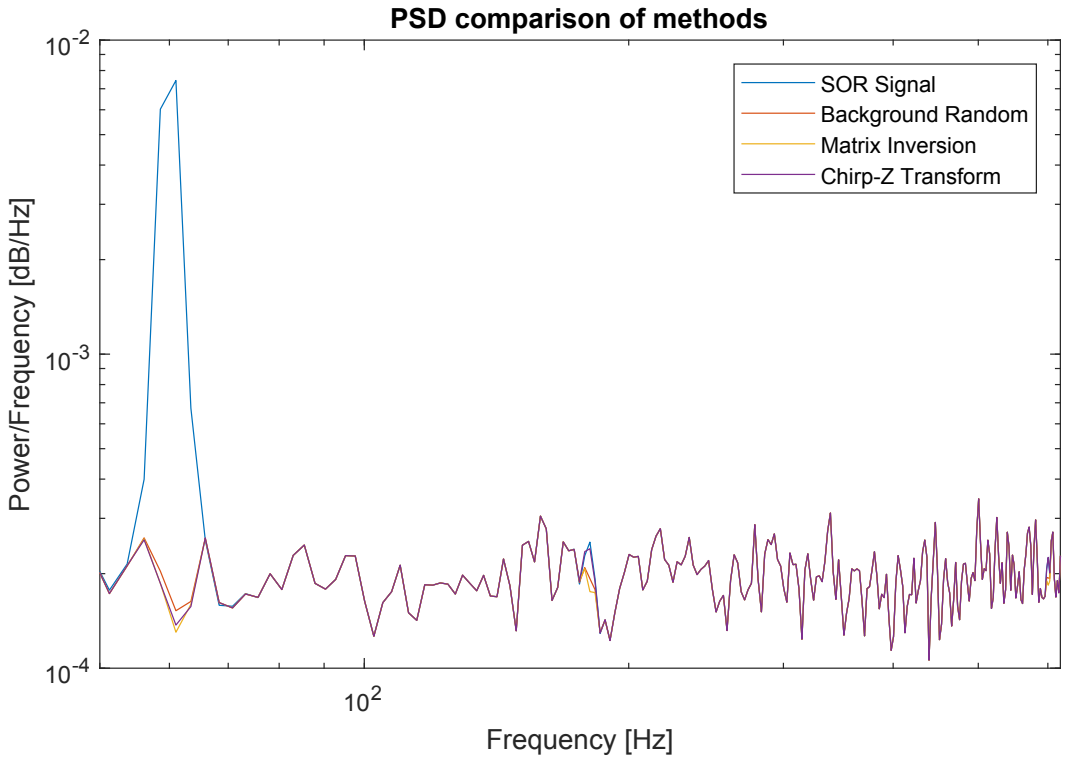


**Figure 24.** Case 2 PSD before and after applying matrix inversion removal.

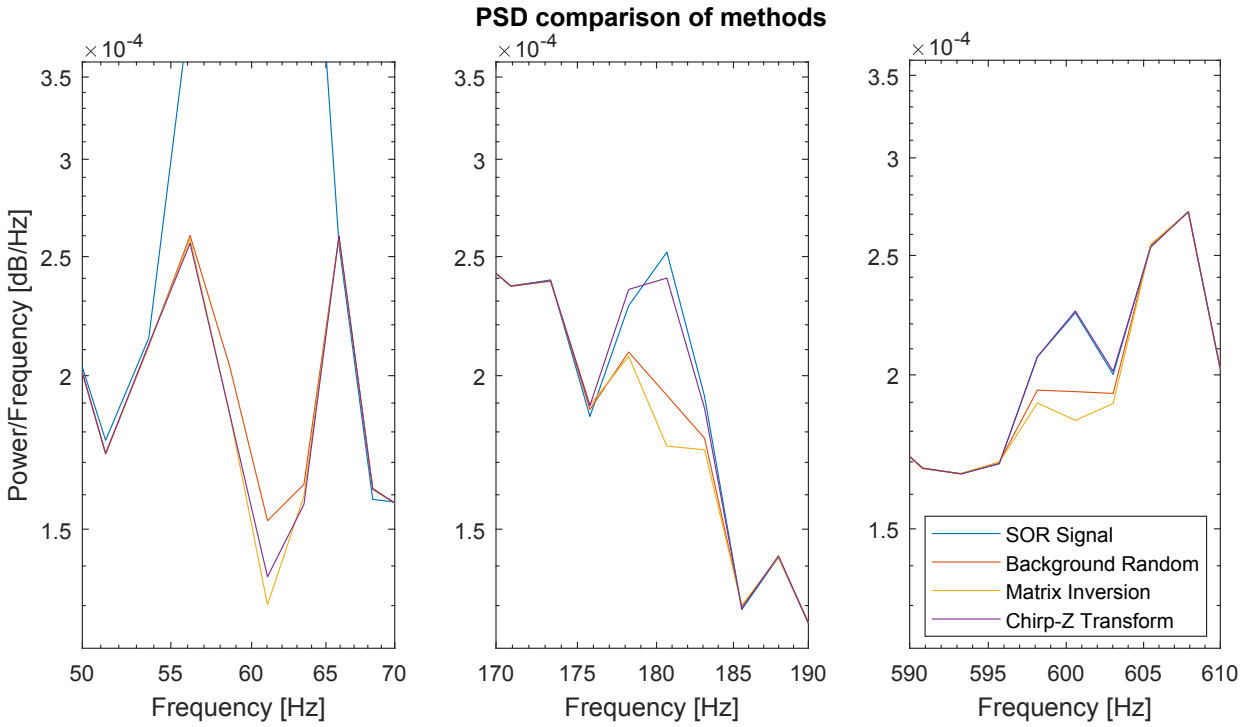


**Figure 25.** Case 2 magnified view of remaining sine tones.

**Table 5.** Case 2 results.

| | Tone | Actual | Matrix | Chirp |
|---|---|---|---|---|
| **Frequency (Hz)** | 1 | 60 | 60.0003 | 59.9958 |
| | 2 | 180 | 180.0184 | 180.1063 |
| | 3 | 600 | 600.0086 | 602.8273 |
| **Amplitude** | 1 | 0.25 | 0.261 | 0.261 |
| | 2 | 0.02 | 0.0241 | 0.0237 |
| | 3 | 0.01 | 0.0180 | 0.00233 |
| | | | | |
| **COV** | **Tone** | **Before** | **After (Matrix)** | **After (Chirp)** |
| | 1 | 0.07122 | 0.5269 | 0.5205 |
| | 2 | 0.4590 | 0.4562 | 0.4976 |
| | 3 | 0.4570 | 0.4125 | 0.4411 |

Because Test Case 2 is a much shorter time history than Test Case 1 the frequency resolution is much higher at 0.0333 Hz. The largest deviation in frequency was 180.0184 Hz, which is still within the resolution limit. It is believed that the inversion method worked better for this case because the FFT method obtained accurate values for the tonal frequencies even at very low SRR. The chirp-z calculated frequencies were outside the required frequency resolution except for the 60 Hz tone. This is the most likely reason the chirp-z method was unable to remove those tones.

The usefulness of the COV metric begins to fall apart at low SRR as shown in Table 5. At 60 Hz the COV before the process was still relatively small which is suggestive of sinusoidal content. After the removal process, the signal at 60 Hz reached the expected COV value of approximately 0.5227. However, the COV for the signal at 180 Hz and 600 Hz actually decreased after the sine removal process.

The result is that without any prior knowledge of the random signal floor, the 180 Hz and 600 Hz tones would be virtually indistinguishable from the random signal. Although the matrix inversion method successfully removed the tones, this success was evaluated with knowledge of the true solution. Without the random signal floor, there is no effective quantitative or qualitative metric to determine if the tones were originally present, or if the tones were successfully removed.

### *4.3.1. Case 2 Iterative Frequency Metric Study*

Both iterative convergence metrics, the sine amplitude and RMS, were tested against Case 2 using the matrix inversion solver. The goal of the iterative solvers as discussed in 2.4.3 is to determine the frequency at which the most sinusoidal content is removed by the matrix inversion. The results of both iterative metrics is shown in Figure 26.

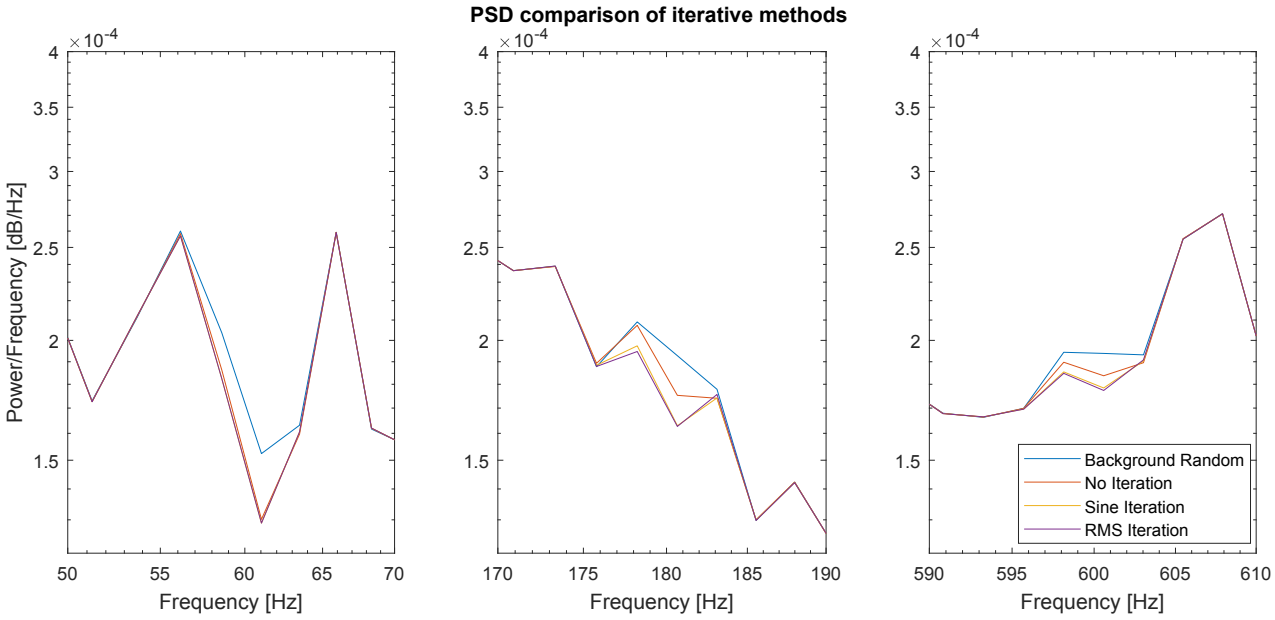


**Figure 26.** Comparison of iterative frequency solvers and original method.

The figure shows that both iterative methods removed more of the peak in the PSD than the original matrix inversion. The sine-optimized iteration and RMS-optimized iteration were roughly equal in effectiveness, although the sine-optimized iteration is much less computationally intensive. However, like the original matrix inversion results these tools removed more content from the signal beyond just the sine tones. The frequencies and amplitudes selected by the iterative solvers are shown in Table 6 in comparison to the original matrix inversion results. Note that although the relative metrics (sine amplitude, RMS) were optimized, the corresponding frequencies and amplitudes were often farther from the true values than the original FFT estimate.

**Table 6.** Case 2 iterative frequency results.

| | Tone | Actual | FFT (no iteration) | Sine Optimization | RMS Optimization |
|---|---|---|---|---|---|
| **Frequency [Hz]** | 1 | 60 | 60.0003 | 60.0002 | 60.0002 |
| | 2 | 180 | 180.0184 | 179.9803 | 179.9636 |
| | 3 | 600 | 600.0086 | 600.0419 | 600.0586 |
| **Amplitude** | 1 | 0.25 | 0.261 | 0.262 | 0.262 |
| | 2 | 0.2 | 0.0241 | 0.0242 | 0.0241 |
| | 3 | 0.1 | 0.0180 | 0.0183 | 0.0183 |
| | | | | | |

| | Tone | Before | COV FFT | COV Sine | COV RMS |
|---|---|---|---|---|---|
| **COV** | 1 | 0.1127 | 0.5269 | 0.5602 | 0.5602 |
| | 2 | 0.4332 | 0.4562 | 0.4952 | 0.4594 |
| | 3 | 0.4570 | 0.4125 | 0.4195 | 0.4238 |

## 4.4. Results: Test Case 3

Both removal methods (matrix inversion, CTZ) were applied to Case 3. Band pass filtering was used in each case. The FFT tool was used for the matrix inversion method. The iteration tool was not used in the main case but was applied to the matrix inversion solver in a subcase described in Section 4.4.1.

The results for both methods are relatively similar, although the matrix inversion method removed more of the sine tones. Both methods removed the tone at 60 Hz. However, neither method removed much of the tones at 180 Hz, 300 Hz, or 420 Hz. These results are shown in Figure 27. The parametric results are tabulated in Table 7.

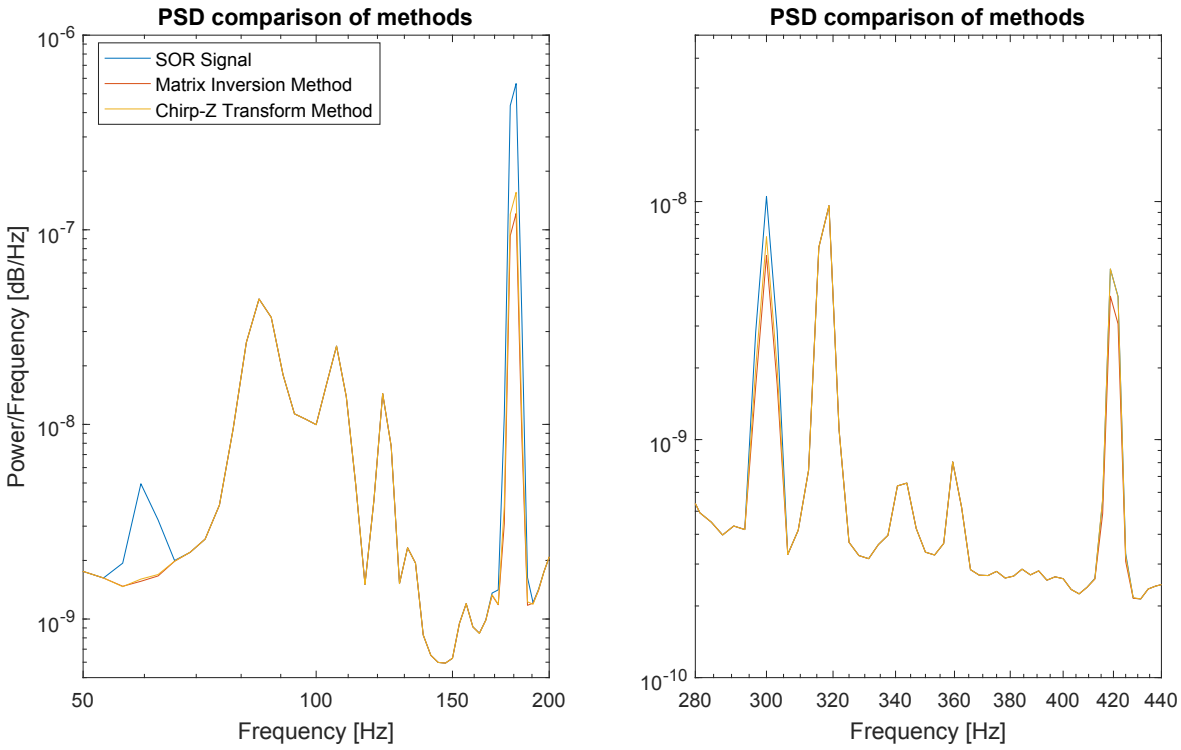


**Figure 27.** Case 3 PSD before and after for each method.

**Table 7.** Case 3 results.

| | Tone | Matrix | Chirp |
|---|---|---|---|
| **Frequency** | 1 | 59.9972 | 59.9986 |
| | 2 | 179.9917 | 179.9944 |
| | 3 | 299.9869 | 299.9917 |
| | 4 | 419.9902 | 419.9917 |
| **Amplitude** | 1 | 0.002 | 0.002 |
| | 2 | 0.0024 | 0.0024 |
| | 3 | 0.003 | 0.003 |
| | 4 | 0.002 | 0.002 |

| | Tone | Before | After (Matrix) | After (Chirp) |
|---|---|---|---|---|
| **COV** | 1 | 0.3298 | 0.5119 | 0.5125 |
| | 2 | 0.0226 | 0.6430 | 0.6853 |
| | 3 | 0.1902 | 0.5029 | 0.5817 |
| | 4 | 0.1156 | 0.5905 | 0.5864 |

The two methods obtained slightly different frequencies. The amplitudes are the same between the two methods. This suggests that the reason the matrix inversion performed better is because the frequency estimate was better, and that the removal of the tone is very sensitive to picking the correct frequency.

The initial COV values support the theory that these frequencies contained sinusoidal line noise because they are close to the theoretical COV value for sinusoids (although the initial COV for the 60 Hz bandpass filtered signal is the least sinusoidal of the raw signals. However, despite the presence of narrowband spikes in the corrected PSD, which suggests that there is still tonal content remaining, the COV values and peak distributions increased towards the ideal Rayleigh value after the removal process which suggests that much of the content was successfully removed.

The peak distributions and the resulting Rayleigh fits at each frequency are shown in Figure 28 through Figure 31.

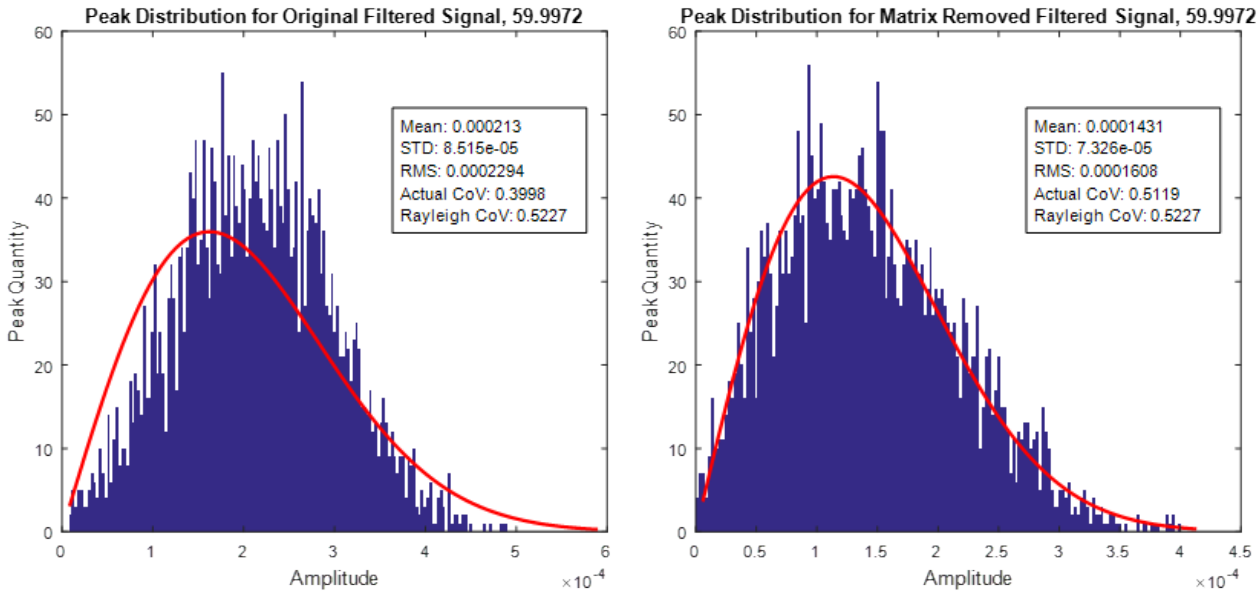


**Figure** 28**.** Case 3 PDFs before and after removal, 60 Hz.

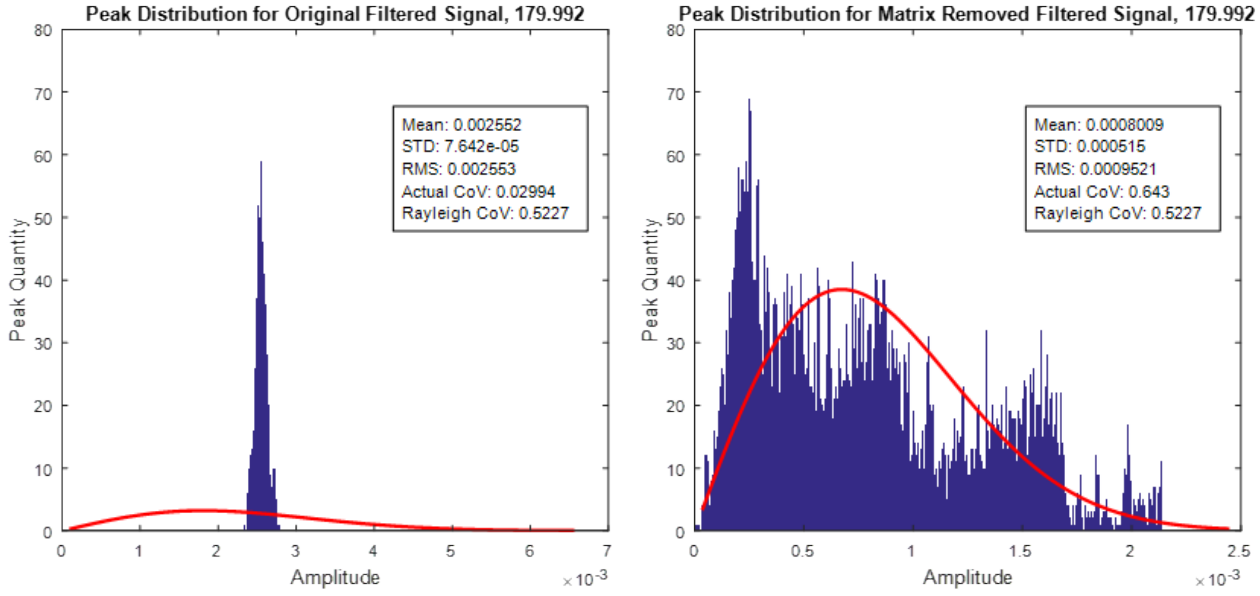


**Figure 29.** Case 3 PDFs before and after removal, 180 Hz.

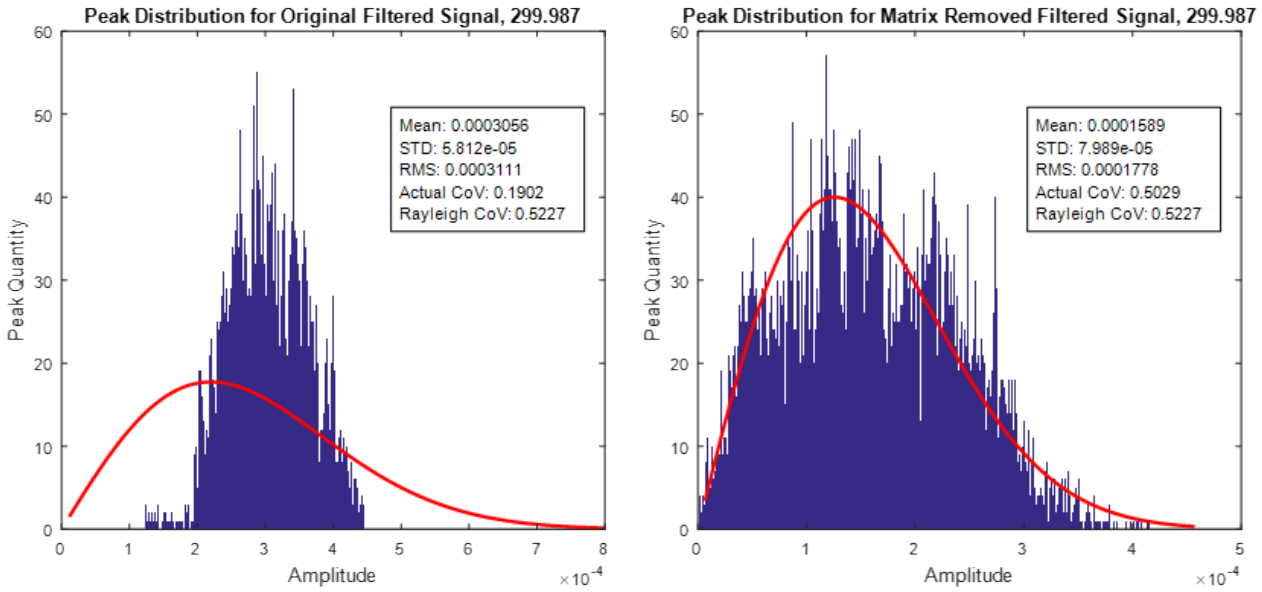


**Figure 30.** Case 3 PDFs before and after removal, 300 Hz.

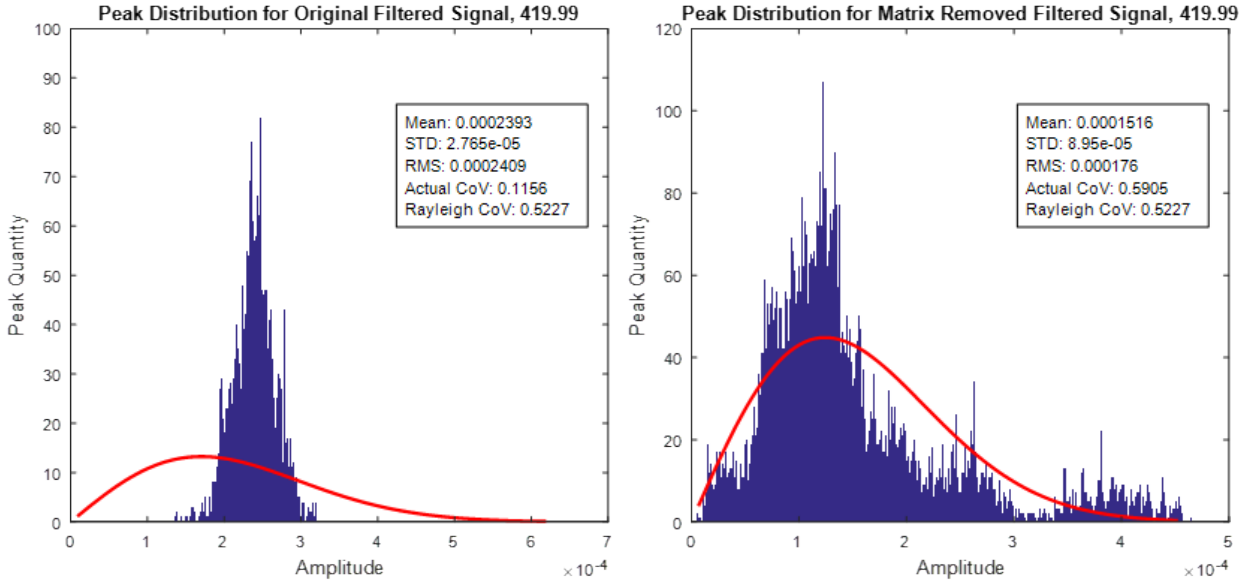


**Figure 31.** Case 3 PDFs before and after removal, 420 Hz.

All frequency bands moved from a characteristic tonal distribution (a large spike at a single amplitude) to a more random Rayleigh distribution after sine removal. These results, combined with the COV values, suggest that the majority of sinusoidal content was removed despite the peaks remaining in the PSD.

The Case 3 data came from an acoustic test involving over one hundred of electrodynamic speakers. One possible reason there are still peaks in the PSD is that there are multi-phased tones present at these frequencies. Another possible explanation might be multiple 60 Hz line noise sources. Differences in cabling length for the various sources could have resulted in small phase shifts between the various sources. Either possibility would result in multiple sinusoids with different phases but the same frequency are overlapping in the signal, and neither removal method would be successful in removing this content.

Another possible explanation is that there are additional tones nearby the 60 Hz harmonics that are responsible for the in ability to identify a single sine tone. An examination of the FFT in the 420 Hz band shows multiple peaks (shown in Figure 32), which may be caused by several sine tones of similar frequency overlapping.

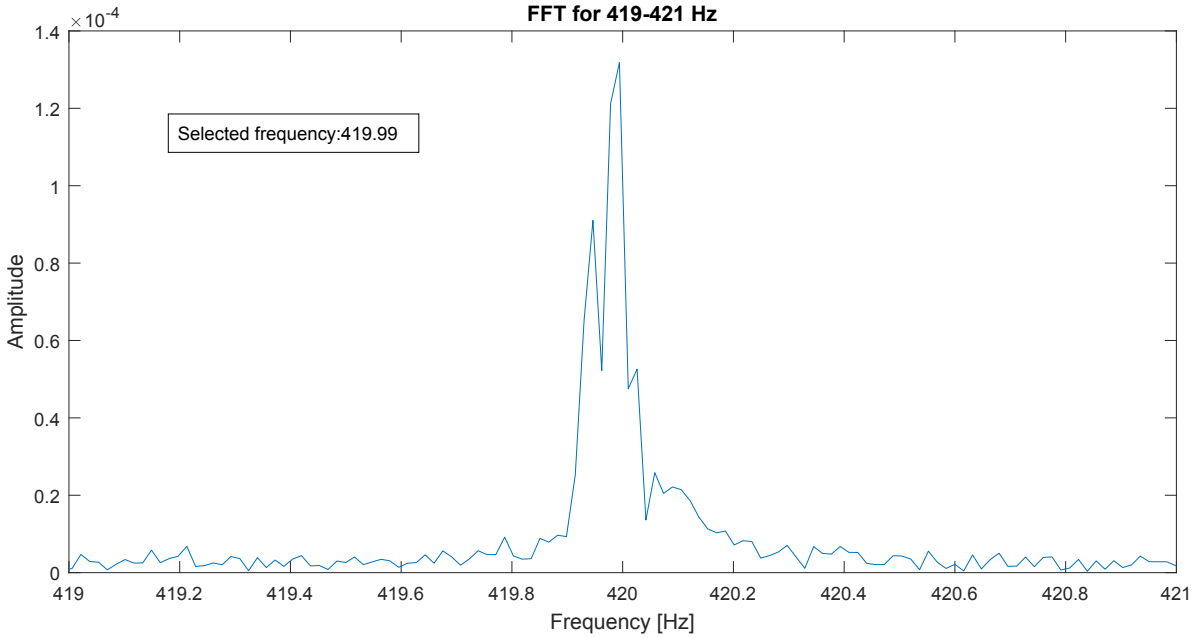


**Figure 32.** Case 3 FFT peaks near 420 Hz.

### *4.4.1. Case 3 Iterative Frequency Results*

The iterative techniques slightly increased removal of the 300 Hz and 420 Hz tones, as shown in Figure 33. The iteration had no effect on the 60 Hz or 180 Hz results. The RMS optimized iteration was able to remove the most content from the PSD.

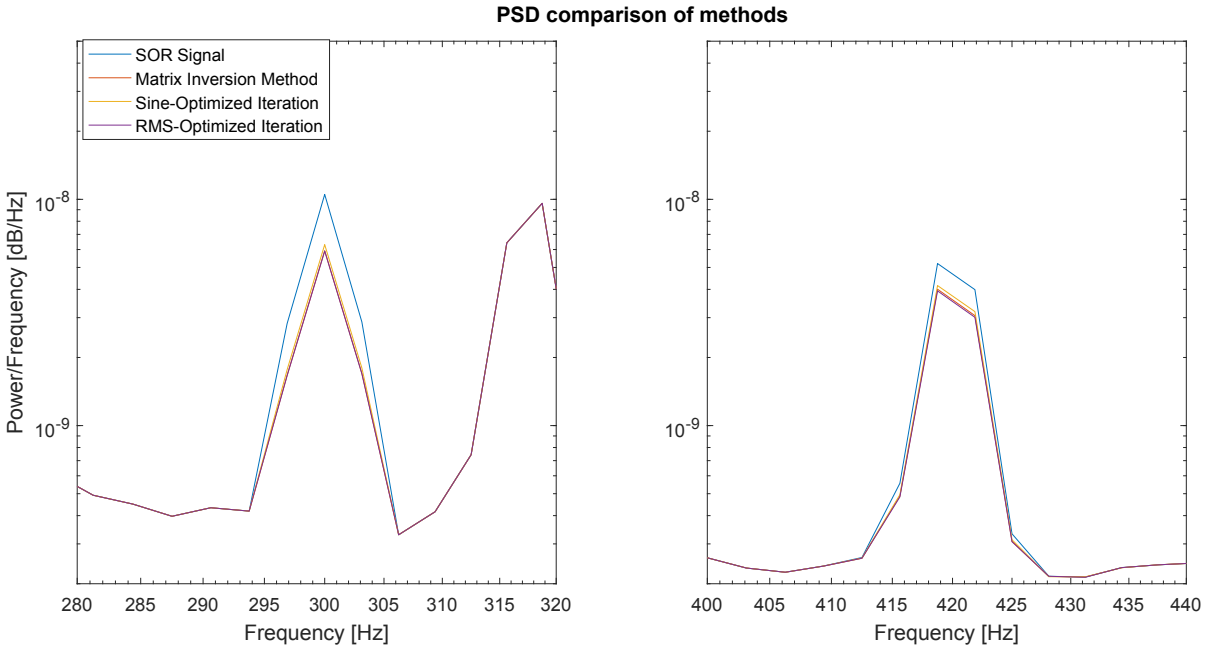


**Figure 33.** Case 3 comparison of iterative methods.

The selected frequencies from both optimization metrics are compared with the original FFT frequency in Table 8.

**Table 8.** Case 3 iterative frequency results.

| Tone # | FFT Frequency (baseline) | Max Sine Amplitude | Min RMS |
|---|---|---|---|
| 1 | 59.9972 | 59.9982 | 59.9982 |
| 2 | 179.9917 | 179.9927 | 179.9913 |
| 3 | 299.9869 | 299.9892 | 299.9865 |
| 4 | 419.9902 | 419.9859 | 419.9939 |
| | **COV Before** | **COV Sine** | **COV RMS** |
| 1 | 0.3998 | 0.5043 | 0.5043 |
| 2 | 0.0299 | 0.7157 | 0.6091 |
| 3 | 0.1902 | 0.5372 | 0.4973 |
| 4 | 0.1156 | 0.5229 | 0.5792 |

These results show that the original FFT frequency was already accurate, as the iterative results provide only a marginal decrease in the PSD peaks.

# 5. FUTURE WORK

An area of interest for future examination is multi-phase sinusoids. This form of signal may explain the removal results for the 180 Hz tone in Test Case 3 as described in 4.4. Multi-phase signals are composed of two or more tones of the same frequency but different phase shifts relative to one another. A common electrical application of this is three-phase power, which is comprised of three sine tones 120° apart from one another in phase. An example of a three-phase power signal is shown in Figure 34.

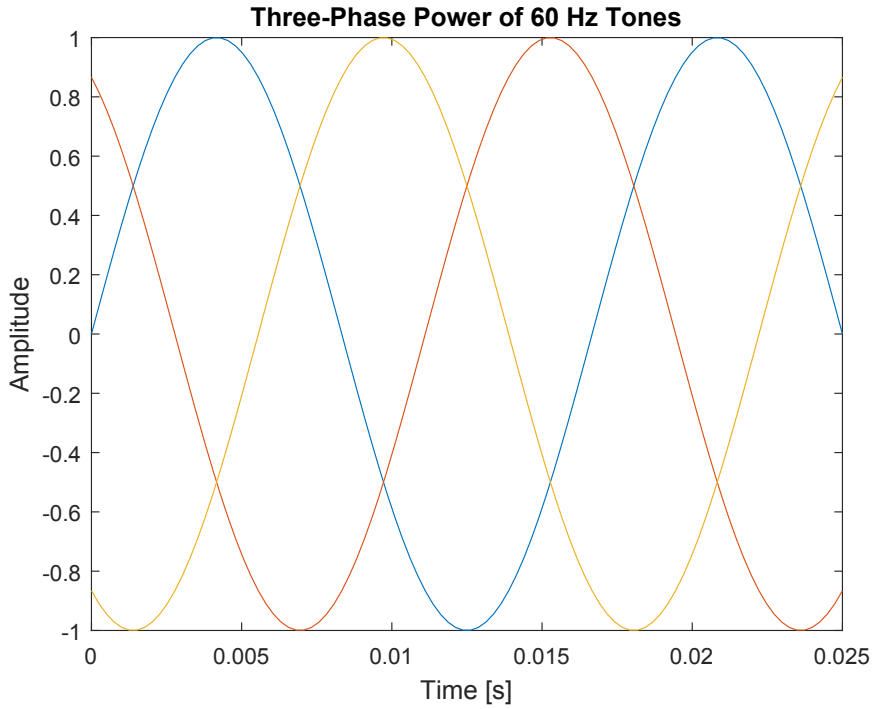


**Figure 34.** Three-phase power signal with sine tones 120° apart in phase.

Because of the common use of three-phase power in electrical systems, it is possible that this could be a source of line noise in the Case 3 signals. When plotted in a PSD, the three-phase power contains a peak at the frequency of the tones. As shown in Figure 35, this matches the appearance of the 180 Hz peak in the Case 3 data.

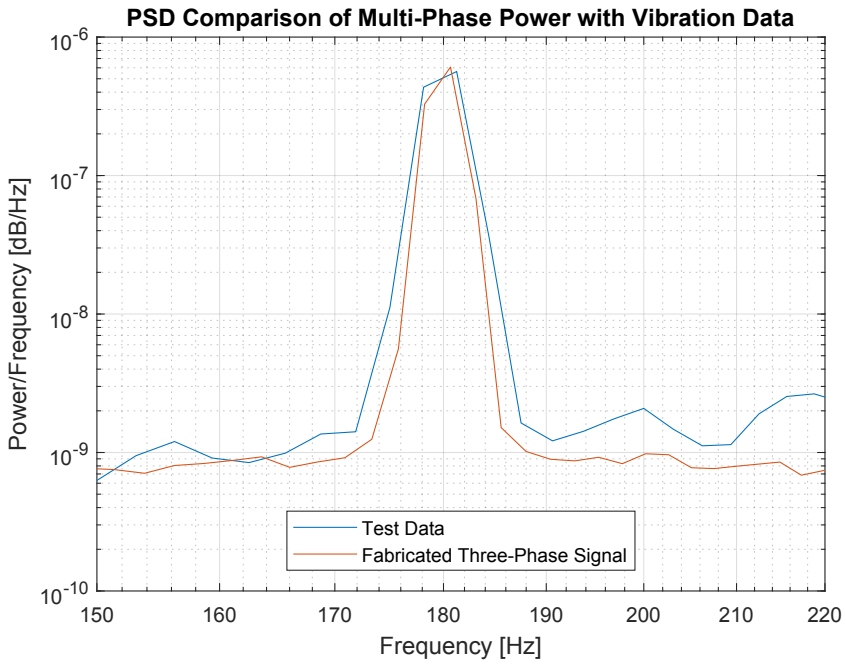


**Figure 35.** Comparison of three-phase power PSD (lower curve) and Test Case 3 (upper curve).

When the matrix inversion removal method is applied to this three-phase signal, it cannot remove the entire peak because of the signal's multi-tone nature. These results are shown in Figure 36. Note the similar to the Test Case 3 results.

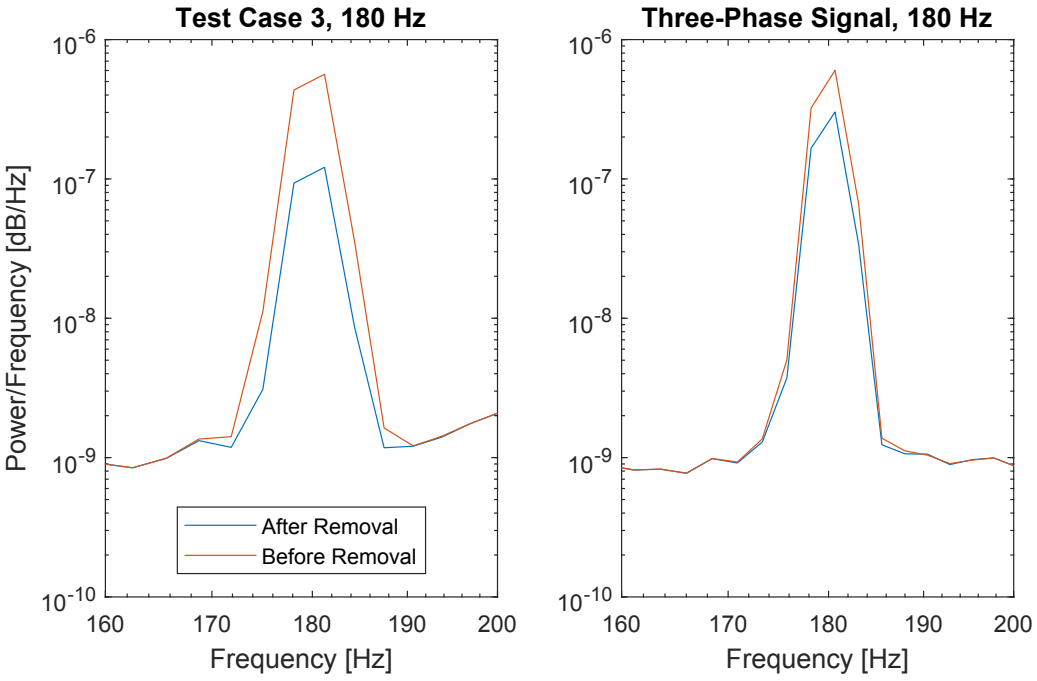


**Figure 36.** Sine removal applied to Test Case 3 and three-phase signal at 180 Hz.

# 6. CONCLUSIONS

Both the matrix inversion and chirp-z transform sine removal methods are mathematically sound and can easily remove sine tones from random signals on theoretical data. Both methods are effective when the sine amplitudes are large; as the SRR decreases below 0.1, the matrix inversion method outperforms the chirp-z. As the SRR approaches 0.01, the matrix inversion method begins to remove more signal content than the sine tone itself, but is still relatively effective.

Similarly, the COV metric to measure the presence and removal of sine tones was effective for SRR above 0.1. At SRR < 0.05, the COV values became unpredictable and in some test cases the removal of the sine tone actually decreased the signal COV rather than increasing it as expected. This, in combination with the decreasing effectiveness of the removal methods at SRR < 0.1, suggests that these methods should only be applied when the SRR is at least 0.1.

Band pass filtering the signal prior to application of either method significantly improves results. Implementing two separate filters to attenuate different regions of the frequency spectrum (local and far frequencies) allows more signal content outside of the frequency range of interest to be removed prior to application of the matrix or CZT solvers.

The optimization metrics used to iteratively determine the tonal frequency are functional at high SRR, with the RMS metric providing the best frequency estimate. As the SRR approaches 0.01, the iterative technique also loses accuracy and usefulness. The FFT method of determining tonal frequency is still very accurate for SRR above 0.01.

For the Case 3 data, both removal techniques were moderately effective but the matrix inversion performed best. The resulting PSD showed that not all of the tonal content was removed at 180 Hz, 300 Hz, or 420 Hz. However, the COVs and PDF plots at each tone showed that a significant portion of the content was removed despite the PSD plot results. The failure to remove the complete tonal content at those frequencies may be a result of multi-phase tones in the signal which overlap at the same frequencies. Further effort is required to fully identify the cause and to solve this issue.

## REFERENCES

Oppenheim, A. V., and Schafer, R. W., 1989, *Discrete-Time Signal Processing.* Prentice-Hall, Upper Saddle River, NJ

# APPENDIX

We performed an empirical study on the accuracy of Equation (15), reproduced below:

$$f_{est} = \frac{P_{n-1}f_{n-1} + P_n f_n + P_{n+1}f_{n+1}}{P_{n-1} + P_n + P_{n+1}}$$

As described in Section 2.4.1, this equation estimates the primary frequency of a signal after being Fourier-transformed. The frequency at the peak amplitude of the transformed signal as well as the frequencies of the adjacent points are combined in a weighted average to form the estimated frequency of the signal. Figure 9 in the aforementioned section shows a visual representation of the point selection.

To verify the validity of this estimation method, we performed a study of the equation's accuracy for small changes in frequency. We created a pure sine tone with unit amplitude. The FFT method has a resolution related to the length of the time history – we created a 100 second signal with a sample rate of 10,000 Hz for a signal 1,000,000 samples long. This gives the FFT a resolution of 0.01 Hz. To verify that Equation (15) could accurately determine the sine frequency within this resolution, we generated a range of frequencies from ± 0.01 Hz of the base frequency. At an interval of 0.0001 Hz this results in 200 different frequencies. The percent error that resulted when the FFT method and Equation (15) were applied is shown in Figure 37 for the normalized frequency range.

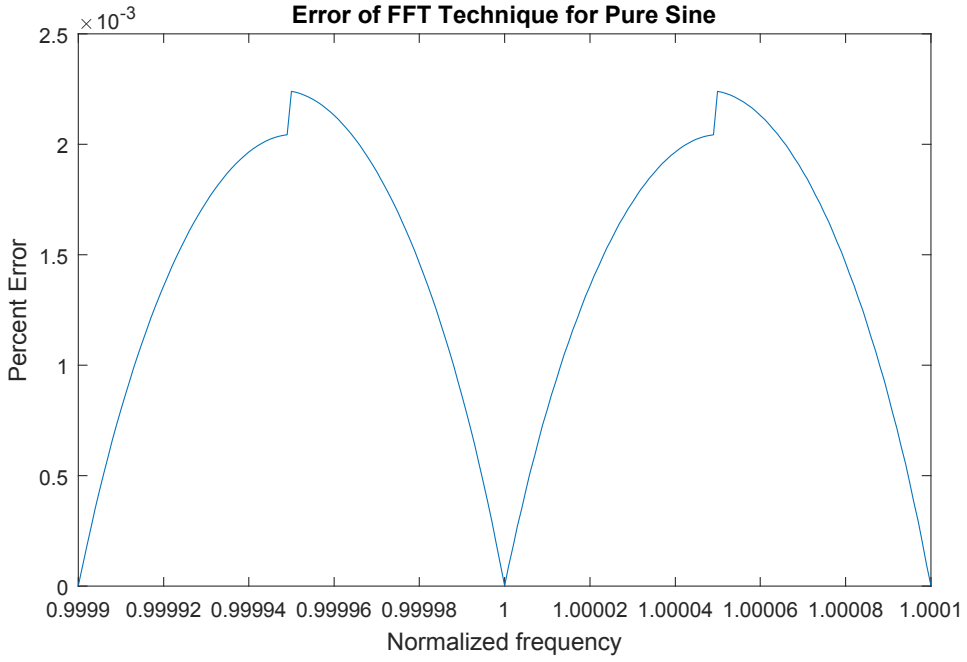


**Figure 37.** Error in frequency identification inside the FFT resolution range.

These results show that while there is no error when the frequency aligns with the FFT resolution, the error inside the ± 0.01 Hz range is nonzero. However, with a maximum value of approximately 0.0022%, this is still negligible.

We also performed an empirical study of the equation accuracy for a range of frequencies and amplitudes. We created SOR signals with an RMS value of 1 for the random component. For the sine component, we selected the amplitudes 0.01, 0.1, 0.5, 1, and 2 which will help demonstrate the equation's accuracy for low and high SRR. Because the RMS is 1, the SRR is equal to the sine amplitude. Frequencies of the sine component ranged from 15 to 1000 Hz with a step size of 5 Hz. This results in 198 different frequencies, each with 5 amplitudes, for a total of 990 different SOR signals. For each SOR signal we applied a band pass filter at the true frequency of the sine tone, then applied an FFT and used Equation (15) to attempt to identify the frequency. This identified frequency was compared to the true frequency to determine the error. After this was done for every selected frequency in the range, this study was repeated for a different sine amplitude. The results of this study are shown in Figure 38 and Figure 39.

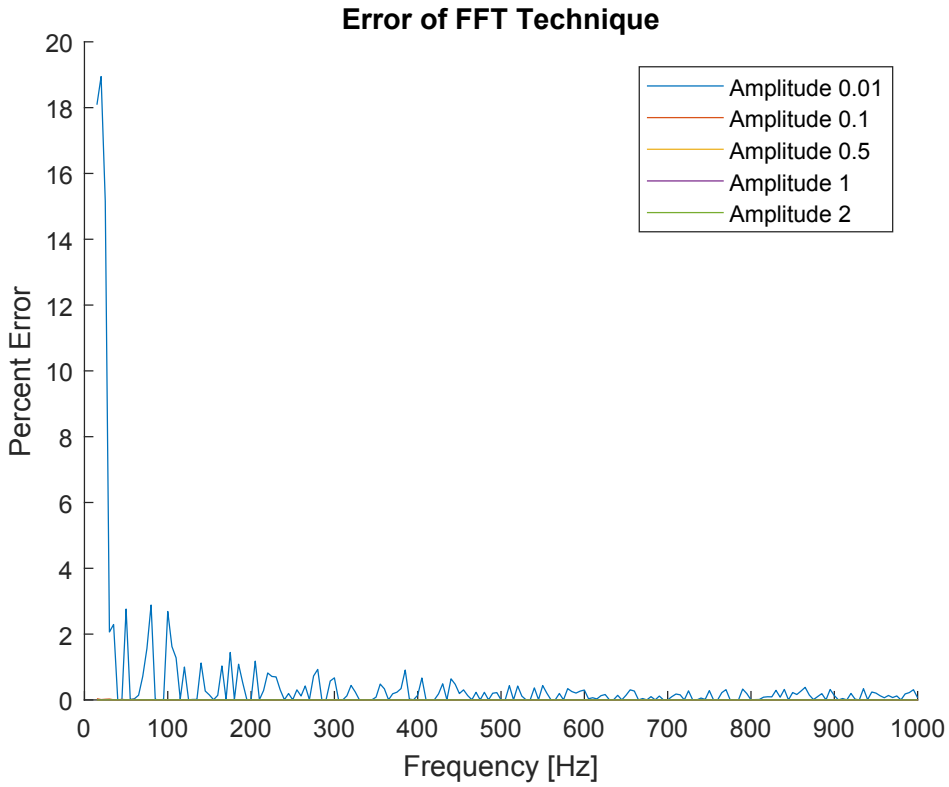


**Figure 38.** Error of frequency identification for ranging sine amplitudes.

As Figure 37 shows, the only significant errors occur at low sine amplitudes. Because the frequency step size was 5 Hz starting at 15 Hz, every selected frequency should be resolvable by the FFT method; unlike before the error should be zero for a pure sine tone. In this case, the error comes from the addition of random noise. For the

amplitude of 0.01, the error is large at low frequencies, but dies off to within 2% by about 120 Hz. However, due to the accuracy required to remove a sine tone this is too large an error, so the best that can be achieved is a partial removal. The higher sine amplitudes have an error close to 0%. A magnified view is presented in Figure 39.

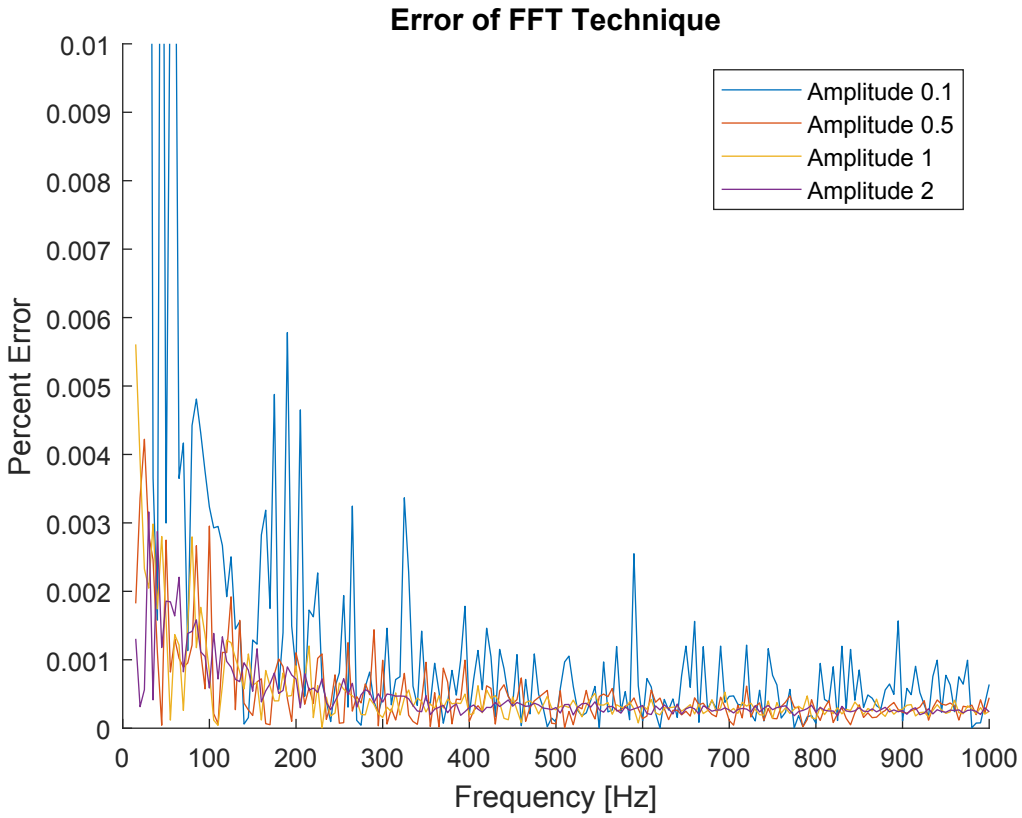


**Figure 39.** Error of frequency identification at higher amplitudes.

For amplitudes greater than 0.1, the error is small, mostly below 0.01%, which is more than sufficient for almost complete sine tone removal. For sine amplitudes above 1 and frequencies above 150 Hz, the error is less than 0.001%. This validates the accuracy of the FFT method and Equation (15) within reasonable limits. For SRR near 0.01, the tonal content is so small that there is virtually no effect in removing it, so it is not significant that the error of the FFT method is large for SRR of 0.01.

## DISTRIBUTION

| | | | |
|---|---|---|---|
| 1 | MS0899 | Technical Library | 9536 (electronic copy) |


Sandia National Laboratories